2 Dimer Models on Anisotropic Lattices

John F. Nagle

Department of Physics, Carnegie-Mellon University, Pittsburgh, Pennsylvania 15213, USA

Carlos S. O. Yokoi

Instituto de Fisica, Universidade de São Paulo, Caixa Postal 20516, São Paulo, Brazil

Somendra M. Bhattacharjee

Institute of Physics, Sachivalaya Marg, Bhubaneswar 751 005, India

PHASE TRANSITIONS
VOLUME 13 ISBN 0-12-220313-5

1 Introduction

In a classic paper in statistical mechanics Kasteleyn (1963) included a short section, consisting only of two paragraphs and a footnote, in which was announced a striking exact result for the phase-transition behaviour of a simple two-dimensional model on an infinite lattice with periodic boundary conditions. The specific heat of Kasteleyn's model is identically zero for all temperatures below the transition temperature. However, when the temperature exceeds its critical value T_K, the specific heat is non-zero and diverges as $(T - T_K)^{-1/2}$ as T approaches T_K from above, as shown in Fig. 1.1.

This behaviour is in marked contrast with that of the two-dimensional Ising model (Onsager, 1944), which has a logarithmic divergence of the specific heat when T_c is approached from either below or above, as is also shown in Fig. 1.1. This contrast in behaviour is especially surprising in view of the fact that both the two-dimensional Ising model and Kasteleyn's model can be solved by the same Pfaffian technique.

The model solved by Kasteleyn that has the aforementioned thermal behaviour is a particular dimer model that will be called the K_1 model. For a small lattice with periodic boundary conditions one microstate of this model is shown in Fig. 1.2.

The next two paragraphs give some background about dimer models and precise definitions of these models for readers who are not familiar with them.

The term *dimer* is an abbreviation for a diatomic molecule. Dimer models were introduced (Fowler and Rushbrook, 1937) as models of physical adsorption of diatomic molecules on crystal surfaces. In that context a general physisorption model for diatomic gases consists of

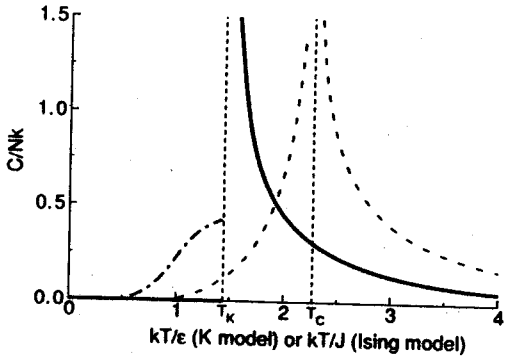

Fig. 1.1 The specific heat C/Nk versus temperature for the K model is shown by the heavy solid line with $C = 0$ below the transition temperature T_K. For comparison, the specific heat for the Ising model on the square lattice is shown by dashed lines. Also, the generic low-temperature specific heat of other models with K-type transitions is shown by the dot–dashed line.

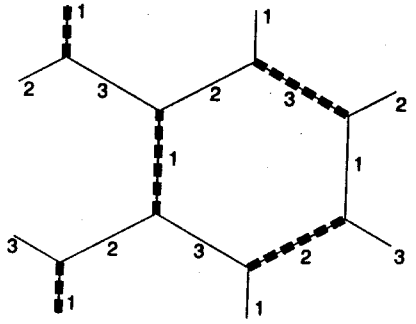

Fig. 1.2 The K_1 model. The three inequivalent bonds are labelled 1, 2 and 3. A particular state is shown with dimers indicated by heavy dashed lines. The energy of this particular state is $2\varepsilon_1 + \varepsilon_2 + \varepsilon_3$.

mixtures of diatomic molecules (dimers) and vacancies (monomers), which is known as the monomer–dimer model. That problem has not been solved by exact methods, even in two dimensions. For all of the exactly solvable dimer models in two dimensions to be discussed in this chapter, the requirement for an allowed state is that each lattice site be covered by one and only one dimer and that each dimer covers two neighbouring lattice sites. Sometimes these dimer models are called close-packed dimer

models to distinguish them from monomer–dimer models, but the shorter term "dimer model" will be employed in this chapter.

In physisorption and in dimer models the energy of a dimer may be different depending upon which pair of neighbours it covers on the underlying crystal surface or lattice. It is often convenient to identify the energy ε_b with the bonds b on the lattice, and it is then said that a dimer covers a bond rather than a pair of lattice sites. The partition function Z for dimer models can then be written as

$$Z(\boldsymbol{z}) = \sum_{\text{microstates}} \prod_{b} z_b^{N_b} . \tag{1}$$

Each activity z_b is simply the Boltzmann factor $e^{-\varepsilon_b/kT}$ for a dimer on a bond of type b with energy ε_b, and the general activity variable $\boldsymbol{z}$ is the set of activities z_b for all different bond types b. The product in (1) is over all of the different types of bonds that may occur in a unit cell. The sum is over all microstates that may be formed by covering each site with exactly one dimer, and N_b is the number of dimers of type b on the entire lattice for the microstate in question.

In terms of the general definitions in the preceding paragraph, the K_1 model illustrated in Fig. 1.2 employs the honeycomb lattice for the topological connection of sites and bonds, but the symmetry is broken by giving dimers different energies ε_b, which correspond to the activities z_b, for the three geometrically distinct bond types, $b = 1$, 2 and 3. Without loss of generality, one may restrict attention to the case $\varepsilon_1 < \varepsilon_2 < \varepsilon_3$. Then, Kasteleyn showed that the transition temperature T_K is given by the relation $z_1 = z_2 + z_3$, i.e.

$$e^{-\varepsilon_1/kT_K} = e^{-\varepsilon_2/kT_K} + e^{-\varepsilon_3/kT_K} .$$

One of the purposes of this chapter is to emphasize that the K_1 model is not an isolated abstract model with bizarre thermal behaviour. It is not isolated because there are many distinct models in two dimensions with the same qualitative thermal behaviour and there are also unsolved three-dimensional analogues. It is not simply abstract because there are physical problems that require the particular features that give rise to this type of thermal behaviour. Two of these problems will be emphasized in this chapter. The first is the main melting transition in biomembranes, which is discussed in Section 9, and extended to amphiphilic monolayers in Section 10. The second is transitions in physisorbed systems involving striped incommensurate phases, which is discussed in Section 11. One of the principal insights offered by this chapter is that these two seemingly disparate types of system are related theoretically through anisotropic dimer models.

Another of the purposes of this chapter is to emphasize that solvable two-dimensional dimer models have only two types of phase transition. These types may be thought of as the Onsager type (with the prime example being the two-dimensional Ising model) and the Kasteleyn type. In the remainder of this review the two different types of transition will be called O-type and K-type transitions, respectively. One of the authors admits to the inconsistency of having earlier (Nagle, 1973b, 1975a) propagated a different name, "$\frac{3}{2}$-order transition", for what is here being called the K-type transition. The rationale for the name $\frac{3}{2}$-order transition was that the free energy has an extra piece proportional to $(T - T_K)^{3/2}$ when $T > T_K$. Also, when approaching the transition from below, the specific heat behaves rather ordinarily, as for approach to a first-order transition, whereas it diverges strongly as $(T-T_K)^{-1/2}$ when approaching from above, as for approach to a transition of higher than first order such as a critical point, so $\frac{3}{2}$-order seemed a descriptive compromise. However, the $\frac{3}{2}$-order name has not caught on. In the area of physisorption this kind of transition is usually named after Pokrovsky and Talapov (1979) for their seminal work on striped commensurate–incommensurate transitions. In this chapter we bow to the convention of naming transition behaviour after people, but suggest that Kasteleyn (1963) deserves priority.

In Section 2 we describe some of the dimer models that have K-type transitions. For purposes of comparison and contrast we also describe some very similar models that have O-type transitions. There are several important properties of these models that are clearly relevant to the transition behaviour. These are identified in Section 3, and the extent to which these properties are valid predictors of the behaviour of anisotropic models is critically examined. In Section 4 some of the details of the solutions are given, with special emphasis on the contrast in the behaviour of the singularities in the integrand of the partition function for the K-type transition compared with the O-type transition. A number of exact results are tabulated in Section 5 for a variety of dimer models. The striking behaviour of the correlation functions for the simplest model with a K-type transition is discussed in Section 6. This behaviour is also dramatically revealed in the finite-size effect as the system size approaches infinity, as discussed in Section 7. Nevertheless, finite-size scaling is obeyed, when "finite-size scaling" is sensibly redefined to account for the strongly anisotropic nature of the models. In Section 8 analogous three-dimensional models with predicted K-type behaviour are discussed.

Sections 2–8 focus upon the statistical mechanics of the K-type transitions. The focus in the remaining three sections is upon two physical applications. The first involves anisotropic chain-melting phase transitions

that occur most notably in lipid bilayer membranes, which are discussed in Section 9. It should be emphasized, however, that this application also leads to a fundamental theoretical development that enhances understanding of the phase diagram of models with K-type transitions, as is discussed in Section 10 in the context of monolayer systems consisting of amphiphilic molecules with many internal degrees of freedom. The second application is to anisotropic-domain-wall, commensurate–incommensurate transitions, where these exactly solvable dimer models provide a firm underpinning to more qualitative theories.

2 Some two-dimensional dimer models

The simplest model with a K-type transition is obtained from the K_1 model by setting the two higher dimer energies, say ε_2 and ε_3, equal to ε. Since there is no loss of generality in setting the lowest dimer energy ε_1 equal to 0, there is then only one effective activity, $z = e^{-\varepsilon/kT}$. This model has been called the K model (Nagle, 1975a). It is appropriate to represent it on the brick lattice shown in Fig. 2.1. Although the brick lattice has the same topology as the honeycomb lattice, it better illustrates the symmetry corresponding to the different dimer energies for the different bonds.

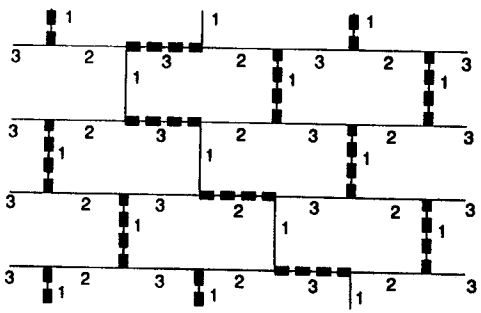

Fig. 2.1 The K model and the K_2 model. The lattice is the brick lattice with three types of distinguishable bonds. A dimer on a type-1 bond has energy ε_1 (= 0) in both models. In the K model a dimer on both type-2 and type-3 bonds has an energy ε. In the K_2 model a dimer on a type-2 bond has energy ε_2 and a dimer on type-3 bond has energy ε_3. The energy for this microstate of dimers shown by bold dashed lines is $8\varepsilon_1 + \varepsilon_2 + 3\varepsilon_3$ for the K_2 model and 4ε for the K model.

Starting from the K model, one may also break the symmetry between the higher energy bonds in a different way from the K_1 model. The way shown in Fig. 2.1 has been called the K_2 model, and was motivated by domain-wall considerations (Yokoi *et al.*, 1986). These three models have the same qualitative phase-transition behaviour already described in Section 1. In fact, the K_2 model has precisely the same transition temperature as the K_1 model, given by the relation, $z_1 = z_2 + z_3$, between the activities.

Let us turn next to a slightly more complex dimer model, which is shown in Fig. 2.2. This model has been very important to the authors because it has helped us to avoid an overly simple characterization of the family of models with K-type transitions.† The exact result for the thermal behaviour of the model in Fig. 2.2 yields a $(T - T_K)^{-1/2}$ divergence in the specific heat as T_K is approached from above, but it also reveals an interesting variation. The specific heat of this dimer model is not zero below T_K but is qualitatively as shown by the dot–dashed line in Fig. 1.1. However, the specific heat does not diverge or have any other non-analytic behaviour as T_K is approached from below, so, from the point of view of modern critical phenomena, it clearly has a K-type transition.

The model in Fig. 2.2 can be characterized by the pattern of dimers in its ground state. This pattern can be described as the repetition of two

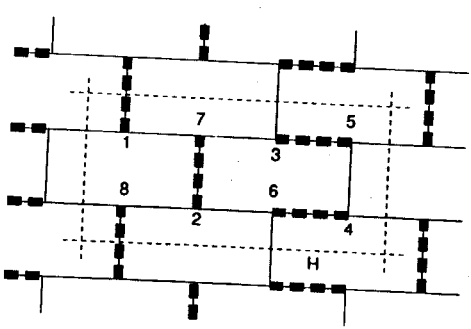

Fig. 2.2 The V^2H^2 dimer model. The positions of dimers in the ground state are shown by heavy dashed lines. Placing a dimer on any other bond costs an energy ε. The light dashed lines show the unit cell, which has a rectangular repeat pattern and which contains eight lattice sites numbered from 1 to 8.

†The V^2H^2 dimer model in Fig. 2.2 was discovered by Nagle and Allen (1971) through a study of proton ordering in a real ferroelectric material, NaH_3SeO_3, although it was shown in that paper that this dimer model is inappropriate for this material. More-appropriate models were discussed in the original paper and by McMullen *et al.* (1982).

columns of vertical dimers followed by two columns of horizontal dimers. A convenient notation for this pattern is VVHH or V^2H^2. In this notation the simple K model becomes just V. Clearly, a whole family of models can be generated simply by writing various products of V and H^2. This family will be called the VH family. The unit cells and the dimer configurations of the ground states of a few of these models are shown in Fig. 2.3. The size of the unit cell, N_{UC}, can be deduced from the VH notation by multiplying the sum of the exponents by two. The density of vertical dimers in the ground state, ϱ_{vg}, is given by the sum p of the exponents of V divided by the sum $p+q$ of all exponents. In order to appreciate the variety and also the common features of models with K-type transitions, a number of these models will be considered explicitly, including V, V^4H^2, V^3H^2, V^2H^2, $V^3H^2VH^2$, VH^2, V^2H^4, V^2H^6, VH^4 and H^2. This sequence of models is arranged in decreasing order of ϱ_{vg}, but within this list both V^2H^2 and $V^3H^2VH^2$ have $\varrho_{vg} = \frac{1}{2}$, and both VH^2 and V^2H^4 have $\varrho_{vg} = \frac{1}{3}$.

The preceding VH models do not exhaust the possible models on the honeycomb lattice. One variation is to introduce more than two energies

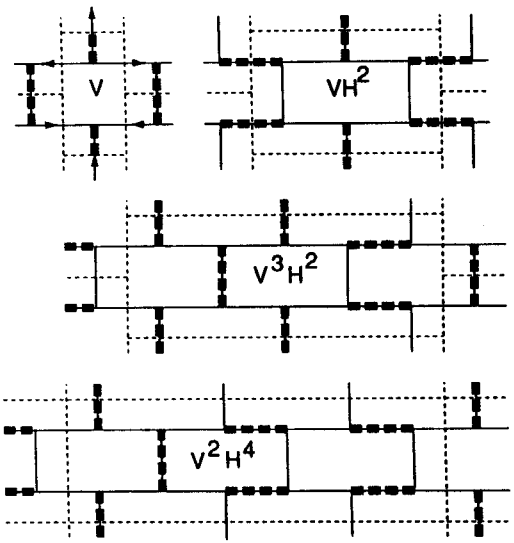

Fig. 2.3 The V, VH^2, V^3H^2 and V^2H^4 members of the VH family. The unit cells, and the way the unit cells are packed on the plane, are indicated by light dashed lines. The positions of dimers in the ground state are shown by heavy dashed lines. Placing a dimer on any other bond costs an energy ε. The arrows on the V model will be used in obtaining the exact solution in Section 4.

for dimers on different types of bonds. For example, in the VH^2 model there are a total of nine different bonds, all of which could have different energies. While there seems little value in considering such a general model, Nienhuis *et al.* (1984) did find it appropriate to introduce a model with six energy parameters in their study of solid-on-solid models of cubic crystal shapes. Their main results and the model of most interest here has two distinct energy parameters. The first of these energies is the same as the energy in the K model, i.e. it favours vertical dimers over horizontal dimers by ε. The second of these energies is the same as the energy in the VH^2 model, i.e. it favours the bold-dashed dimers in Fig. 2.3 by an energy δ. Since this two-parameter model consists of a competition between the K (or V) model ordering and the VH^2 model ordering, we shall call it the VH^2/V model. It will also be of interest to consider a second two-parameter model where the first energy ε corresponds to the energy of dimers in the V^4H^2 model and the second δ corresponds to the energy of the VH^2 model. This model will be called the VH^2/V^4H^2 model.

The K, K_1 and K_2 models and the VH models are all clearly closely related in that the underlying lattice is the three-coordinated honeycomb lattice. However, coordination number three is not a necessary feature for a dimer model to have a K-type transition. Figure 2.4 shows a dimer model on a four-coordinated lattice that is topologically equivalent to the square lattice. In this model a dimer can have three different activities, 1, z or w, depending upon which of three different bond types it covers. In this chapter the model in Fig. 2.4 will be called the SQK model, which

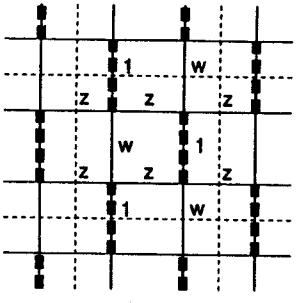

Fig. 2.4 The SQK model. The lattice is isomorphic to the square lattice but has three kinds of distinguishable bonds. A dimer on the type-1 bonds has zero energy, a dimer on the type-w bonds has energy δ and a dimer on the type-z bonds has energy ε. The ground state is shown by heavy dashed lines and the unit cell by light dashed lines.

may be thought of as the staggered quadratic K model.† It reduces to the K model when the activity w goes to zero. The SQK model also reduces to the dimer model on the simple quadratic lattice when $w = 1$. The exact solution to the SQK model shows that it has a K-type transition, with zero specific heat below the critical temperature given by $w + 2z = 1$ and by a specific heat that diverges as $(T - T_K)^{-1/2}$ above T_K.

Neither is lattice coordination number three a sufficient condition that a model have a transition of K type rather than O type. This is illustrated by the 3–12/1 model shown in Fig. 2.5. The lattice will be called the 3–12 lattice because of the appearance of triangles and dodecagons as the basic figures. For $x = w$ the 3–12/1 model is just the dimer model associated with the Ising model on the brick (or honeycomb) lattice (Fisher, 1966). For $x = 0$ this model is isomorphic to the K model of Fig. 2.1 with $z = w^2$ (Bhattacharjee, 1984). It thus provides an example for studying crossover between the O-type and K-type transition behaviour.

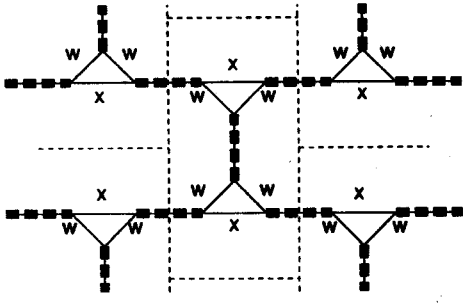

Fig. 2.5 The 3–12 lattice and the unit cell of the 3–12/1 model with dimer activities 1, x and w on the bonds are shown.

Another example of a three-coordinated lattice with an O-type transition is the 4–8/1 model shown in Fig. 2.6. This lattice is called the 4–8 lattice because of the appearance of squares and octagons as the basic figures. The specific heat of the 4–8/1 dimer model is asymptotically symmetrical and logarithmically diverging, just as for the two-dimensional Ising model, and so the 4–8/1 dimer model clearly has an O-type transition, not

†This dimer model has been called the generalized K model (Bhattacharjee and Nagle, 1985), but this name could be confusing because Kasteleyn (1963) also discussed a different generalization of the dimer model on a square lattice; Kasteleyn's generalized model has an O-type transition.

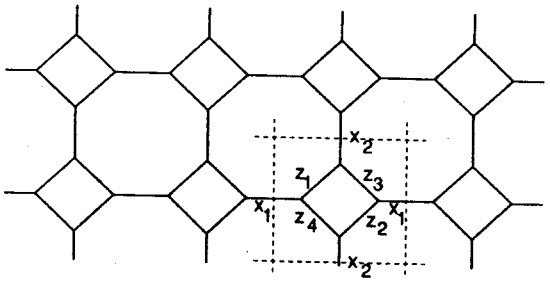

Fig. 2.6 The 4–8 lattice and the unit cell of the 4–8/1 model, for which dimers on the horizontal bonds have activities x_1, dimers on vertical bonds have activities x_2 and dimers on bonds on the squares have activities z_i as shown.

K-type. A model discussed by Salinas and Nagle (1974) to describe the proton-ordering phase transition in $SnCl_2 2H_2O$ (Kitahama and Kiriyama, 1977; Matsuo *et al.*, 1974; Youngblood and Kjems 1979) is a special case of the 4–8/1 model.

Recently, some new models have been discovered (Nagle and Yokoi, 1987) whose phase-transition behaviour is very rich indeed, with multiple transitions, and with interesting correspondences to domain-wall models that will be discussed in detail later. The simplest of these models, which has two transitions of K type, is shown in Fig. 2.7(a), and will be called the 4–8/2/1 model.† It has a unit cell consisting of two "squares" of the 4–8 lattice, arranged in a "staggered" way with each A(B) type square connected only to B(A) type squares. The "2" in the name 4–8/2/1 refers to this feature of the unit cell and the "1" is an arbitrary numbering to distinguish models that are all of the 4–8/2 type. For example, models 4–8/2/2 and 4–8/2/3 are also shown in Figs. 2.7(b) and (c) respectively. At first glance, these three 4–8/2/*i* models are rather similar. However, model 4–8/2/2 has only one transition of O type, and model 4–8/2/3 has no transitions, except in the special case when $z = w$, for which all the 4–8/2 models reduce to a special case of the 4–8/1 model and have one O-type transition.

An interesting variation of the 4–8/2/1 model is shown in Fig. 2.7(d) and will be called the 4–8s/2/1 model. The mere addition of an extra option for placing dimers, no matter how large the energy, changes each of the K-type transitions found in the 4–8/2/1 model into an O-type

†It has been emphasized (Onody and Kurak, 1988) that the 4–8/2/1 model is also a staggered six-vertex model of the sort introduced some time ago (Nagle, 1969a; Baxter, 1973; Wu and Lin, 1975).

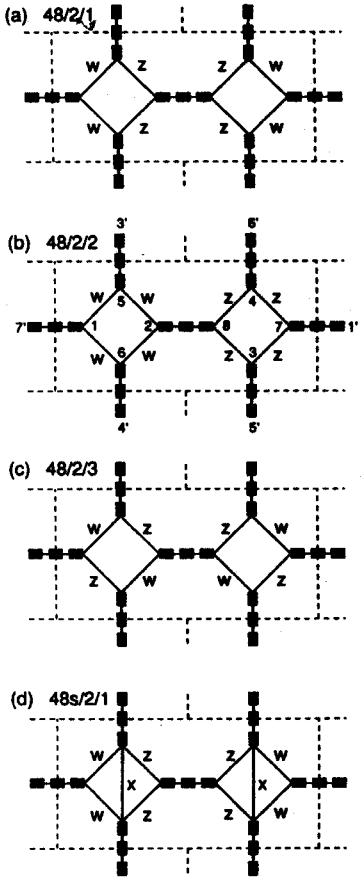

Fig. 2.7 Unit cells for four staggered models based on the 4–8 lattice. The dimer ground state is shown by bold dashed lines. Dimers on other bonds have activities w, z or x as indicated. The numbering of the sites in the 4–8/2/2 model shows how the unit cells are connected.

transition.† In the limit when either z or w becomes 0, the 4–8s/2/1 model reduces to the 3–12/1 model of Fig. 2.5.

We have also explored models with even larger unit cells on the 4–8 lattice. Figure 2.8(a) shows the 4–8/4/1 model, which has a line of Ising transitions when $2zw=1$. In contrast, the 4–8/4/2 model shown in Fig. 2.8(b) has no transition except when $z = w$, for which it reduces to a

†It may also be noted that inclusion of two diagonal bonds in each square leads back, via Kasteleyn (1963), to the dimer representation of the Ising model on the square lattice if all the bonds in the square have the same dimer activity.

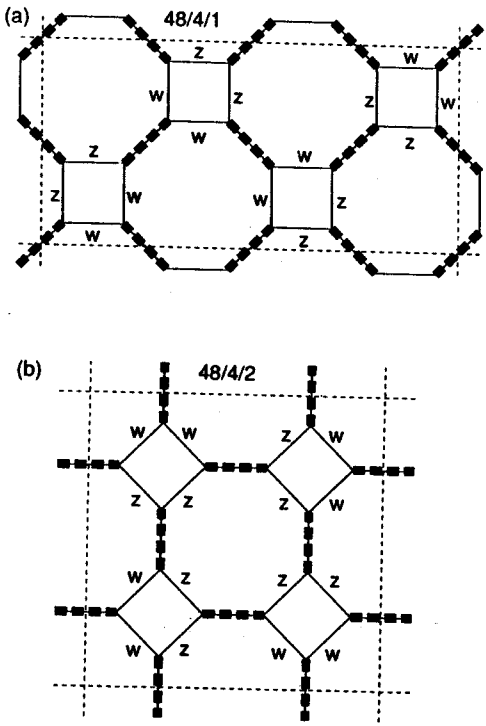

Fig. 2.8 Unit cells for the 4–8/4/1 and 4–8/4/2 models. The dimer ground state is shown by bold dashed lines. Dimers on other bonds have activities w or z as indicated.

4–8/1 model. Additionally, the 4–8/4/1 model has very rich transition behaviour with multiple transitions of both K type and O type when the energy ε of the z-bonds becomes the lowest energy and the ground state becomes frustrated.

The point of this section is that there are many possible dimer models that exhibit interesting thermal behaviour. Clearly, not all the interesting models have been defined and studied, so there is more fun for other workers in statistical mechanics. Nevertheless, it is reasonable at this time to take stock of what is known about these models.

3 Special features of models with K-type transitions

One of the purposes of this chapter is to explore the extent to which one can characterize how models with K-type transitions differ from dimer

models with O-type transitions and from typical spin-type models. This will be done at a number of levels. The focus in this section is upon four particularly simple features that are not shared by spin-type models. There are, however, two somewhat conflicting purposes in this discussion. The first purpose is to explain what these features are so that the reader may appreciate intuitively why K-type transitions occur. The second purpose is to suggest that, important as it is, the intuitive understanding gained from examining these features may not be sufficiently precise to allow reliable predictions whether a new dimer model will have K-type or O-type transitions.

Let us begin by considering the perturbations away from the ground state of the simple K model. Take any type-1 vertical dimer and rotate it around one end onto a horizontal bond. This creates an excluded-volume overlap on a different vertical dimer in a neighbouring row. The new vertical dimer that has been bumped by the original dimer can now be rotated around its other end. Repetition of this bump–rotate process successively involves dimers in successive rows in the lattice, either proceeding upwards or downwards, depending upon how one starts the process. A typical result of this process is shown in Fig. 2.1. Therefore the bump–rotate process can only end at the edge of the lattice for open boundary conditions or by looping the torus and forming a closed cycle of perturbations for periodic boundary conditions. In the limit of an infinite lattice the perturbation involves an infinite number of steps and an infinite energy. As will be justified more fully in Section 11, it is appropriate to call the perturbation shown in Fig. 2.1 a *domain wall*, even though the "domains" on either side of the wall appear identical with each other in Fig. 2.1.

Despite the fact that the domain wall costs an infinite energy, the K model is not completely frozen at all temperatures. Each time a vertical dimer is bumped, it can be rotated in two different ways, so the degeneracy of the domain wall increases as 2^m, where m is the number of rows in the brick lattice. This means that the ground-state contribution to the partition function, which is just 1, becomes negligible compared with the contribution $(2z)^m$, where $z = e^{-\varepsilon/kT}$, from the single domain-wall perturbation when $z > \frac{1}{2}$ amd m goes to infinity. This suggests, but does not prove, that $z = \frac{1}{2}$ might locate the transition temperature; this suggestion is, indeed, verified by the exact solution.†

†The perturbation calculations in this paragraph are very similar to those used to investigate the Slater KDP six-vertex model, which also has an anisotropic forcing constraint. In the case of the Slater KDP model Nagle (1969b) extended those arguments using formal series-expansion arguments to prove rigorously that there is a first-order transition at $kT_c = \varepsilon/\ln 2$ in any dimension. However, a rigorous proof has not been achieved for the K model or

The preceding perturbation calculation reveals an important *conservation property*, which is most easily seen for models on the brick lattice. The property is that the number of vertical dimers in each horizontal row is conserved from row to row. This conservation property is most easily proved by noting that each horizontal dimer excludes one unique vertical dimer in each of two successive horizontal rows of vertical dimers. Therefore for any allowable configuration of horizontal dimers the number of vertical dimers must be conserved in successive rows. The conservation property also clearly implies the forcing constraint for the K_i models.

In the case of the four-coordinated SQK model shown in Fig. 2.4 the preceding conservation property must be generalized. No longer is the number of total vertical dimers per horizontal row conserved. Rather, one must distinguish between those vertical dimers on the lowest-energy bonds with activity 1 and the higher-energy bonds with activity w. A conserved quantity is n_1-n_w, where n_i is the number of dimers per horizontal row on those bonds with activity z_i. Again, this is easily proved by using the fact that for each allowable configuration of horizontal z-type dimers on a row any allowed w-type dimer (one that is not itself excluded by a horizontal z-type dimer) excludes a unique 1-type dimer on the adjacent row of vertical dimers.‡

From the preceding two paragraphs it seems a likely hypothesis that all models with K-type transitions have a conservation property and a relevant domain-wall representation of the microstates of the system. As an example, Fig. 3.1 shows a domain-wall picture of the 4–8/2/1 model. In this figure the domain walls represent those ground state bonds that do *not* have a dimer and those z and w bonds that *do* have a dimer. The 4–8/2/1 model is particularly rich because there are two kinds of domain wall: z-walls, which use z-bonds, and w-walls, which use w-bonds. The two kinds of wall may annihilate when they meet. This means that localized excitation loops, such as the one seen in the upper left corner of Fig. 3.1, which costs $2\varepsilon+2\delta$ in energy, may be formed. In addition, the primarily w-wall seen in Fig. 3.1 has two reversals in direction, at which points it may be thought of as changing into a z-wall and then back to a w-wall or, alternatively, as annihilation/creation pairs. The

its higher-dimensional analogues, although a similar non-rigorous perturbation calculation successfully locates the critical temperature of the K_1 model, the K_2 model and the SQK model. Furthermore, for any of the other VH models shown in Figs. 2.2 and 2.3 there has not even been a simple perturbation calculation to yield the transition temperatures

‡The *full* proof uses the relations, $n_{i,j-1} - n_{i,j} = n_{i+1,j} - n_{i,j} = n_{i+2,j-1} - n_{i+1,j-1} = \cdots = N - n_{i,j}$, where N is the number of lattice sites in each row and $n_{i,j}$ is the number of horizontal dimers in each row. The interested reader may also wish to construct the domain-wall representation for this model.

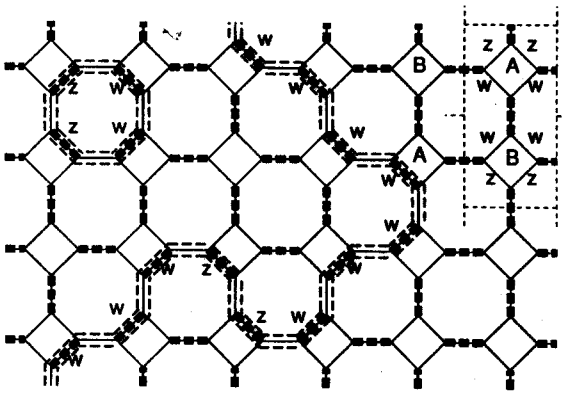

Fig. 3.1 Domain-wall picture of the 4–8/2/1 model. A particular microstate of dimers (bold dashed lines) is shown. Superimposed are domain walls shown as pairs of dashed lines enclosing continuous sequences of bonds on the lattice, with the activities of the high-energy dimers indicated. A unit cell is shown with light dashed lines, with the bond activities and the A/B staggered lattice pattern indicated.

conserved quantity is the number of dimers on z-bonds minus the number of dimers on w-bonds, $n_z - n_w$, which must be the same for each row in a lattice with periodic boundary conditions. While this conservation property may be proved rigorously following the same line of reasoning as the proof for the conserved quantity for the SQK model, it is intuitively obvious from Fig. 3.1 because the net number of z-walls minus the net number of w-walls is conserved from row to row.

Let us now turn to the converse hypothesis, namely that for all models that do not have a K-type transition there is no conservation property. Of course, it is usually more difficult to prove non-existence, but there is an additional feature that forces us to sharpen our notion of the relevance of the conservation property. Consider, as an example, the SCD model, which is the 4–8/1 dimer model (Fig. 2.6) with $x_1 = x_2$ and $z_i = z$ for $i = 1, \ldots, 4$. Just as for the square lattice, the total number of dimers on the vertical bonds is not conserved from row to row. This encourages one to believe in the hypothesis. However, the conservation property elucidated in the preceding paragraph for the 4–8/2/1 model is clearly satisfied by the 4–8 lattice and therefore by the SCD model. This simple example shows that if the concept of a conservation property is to have relevance, it should not only reflect the topological structure of the lattice, but must be refined to reflect the symmetry of the ground state of the model being investigated. Once this is appreciated, it is apparent that the SCD model has no conservation property consistent

with its symmetry, and that it requires breaking the high symmetry of the 4–8 lattice, as in the 4–8/2/1 model, before one would expect to obtain a model with a K-type transition.

The concept that emerged in the preceding paragraph becomes challenged when one considers the 4–8/2/2 model (see Fig. 2.7) and when one evaluates the quantity n_z–n_w with respect to the bond pattern for the 4–8/2/2 model, not for the bond pattern for the 4–8/2/1 model. This quantity n_z–n_w is also conserved from row to row for the 4–8/2/2 model, but this model has only one transition of O type. There is nevertheless a more subtle difference between the 4–8/2/2 model and the 4–8/2/1 model. The quantity n_z–n_w, evaluated with respect to the 4–8/2/2 model, is identically zero. In contrast, n_z–n_w, evaluated with respect to the 4–8/2/1 model, may vary; indeed, its value is a key parameter in describing the phases of the 4–8/2/1 model, as will be discussed later.

The considerations in the preceding two paragraphs impel a more careful discussion of the conservation property for the VH family of dimer models. For the V^2H^2 model Fig. 3.2 shows an excited dimer state superimposed on the ground state, which results in the superposition polygons of Montroll (1964). In the lower left corner of Fig. 3.2 is shown a localized excitation costing 3ε in energy; such excitations account for the non-zero specific heat below T_K. On the right hand side of Fig. 3.2 is shown a domain wall that reverses its direction twice in the middle. A conserved quantity that is specifically relevant to the ground state of the V^2H^2 model is C(m), the net number of domain walls passing through any horizontal row m of the lattice, where a wall that turns around is counted with the opposite sign. C(m) is trivially related to just the total number of vertical dimers, ϱ_v, in each row, which is also the obvious conserved quantity for the K model. The exact solution also shows that the density of vertical dimers remains constant in the low temperature state, whereas ϱ_v decreases steadily in the high temperature state. It must be emphasized, however, that any dimer model has superposition polygons, some of which can be interpreted as domain walls, but that it is not always clear before an exact solution is obtained whether such excitations will ensure a K-type transition.

A final clue to the features that determine whether a model will have a K-type transition (before the exact solution is known) concerns the *spatial anisotropy* of the model. All the known models with K-type transitions have two symmetrically inequivalent principal directions. When the underlying lattice is either the brick lattice or the square lattice the principal directions are the vertical and the horizontal. A further test for the necessity of spatial anisotropy comes from the solution of the VH^2 model, which has three-fold symmetry along the three axes of the honeycomb lattice. This model does not have any transition at finite

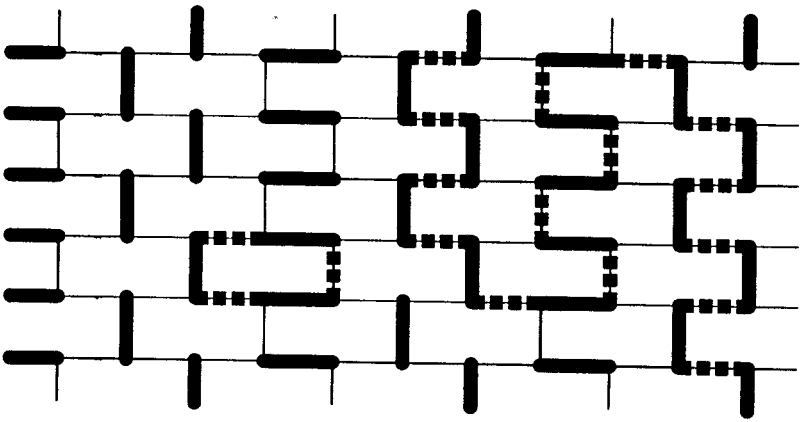

Fig. 3.2 Superposition of ground state dimers (heavy black lines) with excited state dimers (heavy dashed lines) for V^2H^2 model.

temperature, much less a K-type transition. This supports the suggestion that spatial anisotropy is a necessary feature for a model to have a K-type transition. However, spatial anisotropy is by no means sufficient to obtain a K-type transition, as seen by the simple quadratic dimer model. Another pertinent example is the V^2H^4 model. This model is also spatially anisotropic, but the exact solution shows that it behaves similarly to the VH^2 model.

This section has emphasized that there are many clues to whether a given dimer model will have a K-type transition and many properties that are clearly relevant to describing these models. Nevertheless it appears dangerous to espouse any comprehensive theorems that might be proven incorrect by exact calculations, to which it is now logically time to turn in a volume devoted to statistical mechanics. The reader who prefers physical motivation before delving into the intricacies of statistical-mechanical calculations may, however, turn to Sections 9–11 to examine the applications first.

4 Mathematical foundations of the transition behaviour

In this section the method for obtaining the formal integral solution to dimer models in two dimensions is first briefly illustrated. We then enter into a detailed discussion showing how the different kinds of transition behaviour are related to the algebraic structure of the matrix computed by the method.

The exact method of solving dimer problems using Pfaffians was discovered independently by Temperley and Fisher (1961) and Kasteleyn (1961). It was developed and rigorously proved in Kasteleyn's classic 1963 paper, a tutorial chapter has been written by Montroll (1964), and it has been covered in the books by McCoy and Wu (1973) and Thompson (1972). While another derivation of the method would clearly be inappropriate, it is essential to review briefly the results of the method, and this review also should suffice to allow the interested reader to apply the method to new models. The result of applying the method to infinite lattices with periodic boundary conditions† is an exact double-integral expression for the logarithm of the partition function per unit cell (N unit cells) as a function of all the activities in the model, designated by $\boldsymbol{z}$.

$$\frac{\ln Z(\boldsymbol{z})}{N} = \frac{1}{8\pi^2}\int_0^{2\pi} \mathrm{d}\theta \int_0^{2\pi} \mathrm{d}\phi \ln \det \boldsymbol{M}(\boldsymbol{z},\theta,\phi)\,, \tag{2}$$

in terms of the determinant of a matrix $\boldsymbol{M}$, which must be determined specifically for each dimer model.

The simplest illustration of the Pfaffian method is given by the solution of the K model. A unit cell of the K model is shown in Fig. 2.3, where it is identified as the V model. The arrows on the bonds in Fig. 2.3 conform to Kasteleyn's clockwise-odd rule for each elementary "brick" in the lattice. The unit cells are packed in a triangular pattern with six neighbours for each cell. An anti-Hermitian matrix $\boldsymbol{M}$ of dimension equal to the number of sites in the unit cell is constructed according to the following recipe. For each bond joining site j to site k add to the matrix element M_{jk} the product of

the bond activity,

u to the power of the x-coordinate unit cell index of the kth site,

v to the power of the y-coordinate unit cell index of the kth site,

-1 if and only if the arrow on the bond points from k to j.

The functions u and v are related to the angles θ and ϕ in (2) by $u = \mathrm{e}^{\mathrm{i}\theta}$ and $v = \mathrm{e}^{\mathrm{i}\phi}$. For the K model $\boldsymbol{M}$ is a 2×2 matrix consisting of

†It should be noted that the choice of boundary conditions for dimer models on lattices of low coordination number may even affect bulk properties. Trivial examples abound for which the boundary conditions completely determine the dimer state uniquely, and a non-trivial example has been calculated by Elser (1984). While none of these examples represents appropriate open boundary conditions—which would have dangling bonds at the boundary, which could either be or not be occupied by a dimer—even for this more appropriate case it is not proven that the bulk properties are the same as for periodic boundary conditions. It is encouraging, however, that the same results are obtained with periodic boundary conditions when different unit cells and different (θ,ϕ) directions (see below) are chosen, even though the excitations that loop the torus are inequivalent.

zeros on the diagonal and a, and $-a^*$ in the two off-diagonal positions respectively, where $a = v^2 + 2vz \cos\theta$. The v^2 term comes from the bond connecting the upper site in the unit cell shown in Fig. 2.3 to the site in the unit cell directly above with unit-cell index (0,2). The $vz(u + u^{-1})$ terms come from the bonds connecting this same site to the two neighbours in the same row with unit-cell indices $(1, \pm 1)$.

The reader should now be able to obtain the integral expression (2) for any of the dimer models discussed in this chapter or any new models of interest. It should, however, be appreciated that obtaining a formula of the type of (2) is the major step in obtaining exact solutions in the statistical mechanics of cooperative phenomena. This should not be obscured by the relative brevity of the preceding two paragraphs compared with the much greater space devoted to analysing (2) to extract thermodynamic details for specific models. Rather, the simplicity of this step for dimer models in two dimensions is a testimonial to the Pfaffian method. Furthermore, the fact that taking such a step is practically impossible for most models of physical interest places a special emphasis on those models for which exact rigorous solutions can be obtained.

For the K model and for many of the models that will be considered in this chapter $\boldsymbol{M}$ has a simple block structure, consisting of four equal-sized blocks.† The two diagonal blocks consist only of zeros‡. Let one of the off-diagonal blocks be called $\boldsymbol{M}_1$. Since $\boldsymbol{M}$ is anti-Hermitian, the other off-diagonal block is $-\boldsymbol{M}_1{}^*$. Since

$$\ln \det \boldsymbol{M} = 2 \operatorname{Re} (\ln \det \boldsymbol{M}_1), \tag{3}$$

it is only necessary in these cases to display the simpler $\det \boldsymbol{M}_1$ function. While $\det \boldsymbol{M}_1$ is generally complex, $\det \boldsymbol{M}$ is clearly real and positive for all values of its arguments when $\boldsymbol{M}$ is decomposable into two off-diagonal blocks.§ The two integrals in (2) are difficult to obtain in closed form

†The blocks for the K model are just single elements.

‡For example, this is brought about by the numbering of lattice sites shown in Fig. 2.2 for the V^2H^2 model and in Fig. 2.7 for the 4–8/2/2 model. Exceptions to the case discussed in this paragraph are the 4–8/1 model in Fig. 2.6, the 4–8s/2/1 model in Fig. 2.7(d) and any model for which the lattice sites cannot be divided into two sets such that all lattice sites in one set are connected only to sites in the other set, i.e. non-bipartite lattices.

§Even when $\boldsymbol{M}$ is not decomposable into two off-diagonal blocks, $\det \boldsymbol{M}$ is real and positive in all cases that we have encountered. The reality of $\det \boldsymbol{M}$ follows easily from the anti-Hermitian property of $\boldsymbol{M}$ *provided* that the order of $\boldsymbol{M}$ is even; $\det \boldsymbol{M}$ is imaginary if the order of $\boldsymbol{M}$ is odd. The positivity of $\det \boldsymbol{M}$, for even order, is not a general property of anti-Hermitian matrices, even when the matrix is spineless (zeros on the diagonal), as can be seen by a 4×4 counterexample. Thermodynamically, it is necessary that $\ln Z$ be real, but this does not preclude the cancellation of imaginary parts if $\det \boldsymbol{M}$ goes negative or imaginary. Nevertheless, experience indicates that it is reasonable in subsequent discussion to focus upon the case when $\det \boldsymbol{M}$ is both real and positive for all values of z, θ and ϕ.

because of the presence of the logarithm, as is well known from the appendix of Onsager's (1944) famous paper. It is easier to work with the energy E/N or with the densities of dimers $\varrho_{z_b} = N_b/N$, which involve first derivatives of $\ln Z$, such as

$$\frac{E}{N} = \frac{kT^2}{N}\frac{\mathrm{d}\ln Z}{\mathrm{d}T}, \qquad \varrho_{z_b} = z_b \frac{\mathrm{d}}{\mathrm{d}z_b}\left(\frac{\ln Z}{N}\right), \tag{4}$$

which yields integrals like

$$\int_0^{2\pi}\mathrm{d}\theta\int_0^{2\pi}\mathrm{d}\phi\,\frac{\mathrm{Num}\,(z,\theta,\phi)}{\det \boldsymbol{M}(z,\theta,\phi)} \sim \frac{E}{N}, \tag{5}$$

where the Num function in the numerator of the integrand in (5) depends upon which first derivative (which bond b) is being taken.

In the case of the simple K model the integrals in the preceding paragraph are easily obtained, as is now shown. Using (1)–(5), one obtains

$$\frac{E}{N} = \frac{\varepsilon z}{N}\frac{\mathrm{d}\ln Z}{\mathrm{d}z}$$

$$= \frac{\varepsilon}{4\pi^2}\int_0^{2\pi}\mathrm{d}\theta\int_0^{2\pi}\mathrm{d}\phi\,\frac{2z\cos\theta}{\mathrm{e}^{\mathrm{i}\phi} + 2z\cos\theta}, \tag{6}$$

where N is the number of unit cells in the model, which is half the number of lattice sites. Next, the substitution $v = \mathrm{e}^{\mathrm{i}\Phi}$ is made and the integral over v is performed by calculus of residues. For $z < \frac{1}{2}$ the residues at $v = 0$ and at $v = -2z\cos\theta$ sum to zero, giving $E = 0$, so the thermodynamic state of the system consists only of the ground state. For $z > \frac{1}{2}$ the pole at $v = -2z\cos\theta$ is outside the unit circle if $-\Theta < \theta < \Theta$ or if $\pi - \Theta < \theta < \pi + \Theta$, where

$$\Theta = \cos^{-1}\left(\frac{1}{2z}\right). \tag{7}$$

When summed with the contribution from the pole at $v = 0$, the final result is

$$\frac{E}{N} = \frac{2\varepsilon}{\pi}\int_0^{\Theta}\mathrm{d}\theta = \frac{2\varepsilon}{\pi}\cos^{-1}\left(\frac{1}{2z}\right) \tag{8}$$

From this result for the energy,† the free energy can be obtained

†It may be noted that the energy approaches $\frac{2}{3}\varepsilon$ as T approaches infinity. This corresponds to each unit cell, which consists of two sites and one net dimer, having $\frac{2}{3}$ of a horizontal dimer and $\frac{1}{3}$ of a vertical dimer on average.

by integrating with respect to T, and the specific heat is easily obtained by taking the derivative with respect to T, yielding for $T > T_K = \varepsilon/(k \ln 2)$

$$\frac{C}{Nk} = \frac{2}{\pi}\left(\frac{\varepsilon}{kT}\right)^2 \frac{1}{(4e^{-2\varepsilon/kT} - 1)^{1/2}}, \tag{9}$$

which is plotted in Fig. 1.1. This specific heat exhibits the square-root divergence ($\alpha = \frac{1}{2}$) because z varies linearly with T as T approaches T_K from above. The density of horizontal dimers is just $E/N\varepsilon$, and the density of vertical dimers and horizontal dimers sums to unity. Remarkably, this completes the calculation of the thermodynamic properties of the K model. In particular, for this model there is no obvious second intensive thermodynamic variable, such as a magnetic field, a point to which we shall return in Section 10.

As just shown, in the case of the K model the integrals in (5) are easily performed. However, for other models the integrals are more complicated, and in such cases it is very useful to be able to diagnose what kind of analytical behaviour to expect near the critical points without working out a complete formula† or relying exclusively on numerical integration. It is also interesting to see how the mathematical development of the O-type logarithmic singularity differs from the development of the $\frac{3}{2}$-order K type of singularity in terms of the algebraic structure of $M(z,\theta,\phi)$.

The first focal point for answering the aforementioned questions is the investigation of the zeros of det $M(z,\theta,\phi)$, since ln $Z(z)$ can only become non-analytic at values of z_c if the integrands in (2) and (5) are non-analytic at some place in the (θ,ϕ) plane. The zeros of det $M(z,\theta,\phi)$ for the K model follow a pattern that is typical of all models with K-type transitions. It suffices to consider det $M_1 = (e^{i\phi} + 2z \cos\theta)e^{i\phi}$, which has zeros whenever

$$v \equiv e^{i\phi} = -2z \cos\theta. \tag{10}$$

Since the right-hand side of (10) is real, it is clear that zeros in det M can only occur for $\phi = 0$ or π. It is also clear that there are no zeros for $z < \frac{1}{2}$ because the right-hand side of (10) is less than 1. For $z = \frac{1}{2}$ there are two zeros, one at $\theta = 0$, $\phi = \pi$ and one at $\theta = \pi$, $\phi = 0$. As z is taken larger than $\frac{1}{2}$, each of the zeros for $z = \frac{1}{2}$ splits into a pair of zeros, one pair at $\theta = \pm\Theta$, $\phi = \pi$ and one pair at $\theta = \pi \pm \Theta$, $\phi = 0$, where Θ is given by (7). By noting the symmetry of det $M(z,\theta,\phi)$ in the

†For example, in the case of the 4–8/2/1 model M. L. Glasser has shown (private communication) that, although the energy can be expressed analytically, it involves a non-trivial combination of incomplete elliptic integrals of the first and second kinds.

(θ,ϕ) plane, the θ integral in (5) can be restricted to the interval $[0, \frac{1}{2}\pi]$, so only the zero at $\theta = \Theta$, $\phi = \pi$ need be considered. Despite the existence of zeros in det $\boldsymbol{M}$ for $z > \frac{1}{2}$, the thermodynamic functions are analytic, and only become non-analytic at the K-type transition at $z_c = \frac{1}{2}$. Near the critical point det $\boldsymbol{M}$ scales as

$$\det \boldsymbol{M}(z,\theta,\phi) \sim (\theta^2 - t)^2 + \phi^2 , \tag{11}$$

where t is the reduced temperature $(T - T_K)/T_K$.

The form of det $\boldsymbol{M}$ close to its zero in (11) suffices to predict the analytic behaviour of the K-type transition, as we now show. Using (4) and (5), one has

$$\frac{E}{N} \sim \int_0^\delta \mathrm{d}\theta \int_0^\delta \mathrm{d}\phi \, \frac{t - \theta^2}{(t-\theta^2)^2 + \phi^2} . \tag{12}$$

Performing the change of variable $\phi = (t - \theta^2)x$ yields

$$\frac{E}{N} \sim \int_0^\delta \mathrm{d}\theta \int_0^{\delta/(t-\theta^2)} \frac{\mathrm{d}x}{1 + x^2} . \tag{13}$$

The integral over x yields $\tan^{-1}[\delta/(t-\theta^2)]$, which, near the transition when t is small and for θ small, can be replaced by $\frac{1}{2}\pi$ sign $(t-\theta^2)$. For $t > 0$ above the transition the θ integral in (13) may then be split into two parts:

$$\begin{aligned} \frac{E}{N} &\sim \int_0^{t^{1/2}} \mathrm{d}\theta \tfrac{1}{2}\pi + \int_{t^{1/2}}^\delta \mathrm{d}\theta \left(-\tfrac{1}{2}\pi\right) \\ &= \pi t^{1/2} - \tfrac{1}{2}\pi\delta \end{aligned} \tag{14}$$

In contrast, for $t<0$ there is only one integral over the range $[0,\delta]$, which yields $-\frac{1}{2}\pi\delta$. This demonstrates the non-singular nature of the energy below T_K and the square-root temperature dependence above T_K, which yields the $t^{-1/2}$ divergence of the specific heat.

For comparison, we now turn to a discussion of the behaviour of the zeros in models that have O-type transitions with logarithmic specific-heat singularities. As an example, let us consider the special case of the 4–8/1 model, for which $x_1 = x_2 = 1$ and $z_i = z$ for all i. Then

$$\det \boldsymbol{M} = 1 - 4z^2 \cos\theta \cos\phi + 4z^4 . \tag{15}$$

There is only one zero in det $\boldsymbol{M}$, which occurs at $z_c = \frac{1}{2}$ and $\theta = 0 = \phi$. In the vicinity of this zero det $\boldsymbol{M}$ scales as

$$\det \boldsymbol{M} \sim t^2 - \theta^2 - \phi^2 . \tag{16}$$

In order to obtain the asymptotic non-analyticity, we replace det M in (5) by the scaling-form approximation (16). This gives the following contribution from the double integral near the origin ($|t| \ll \delta \ll 1$):

$$\frac{E}{N} \sim \int_0^\delta d\theta \int_0^\delta d\phi \frac{t}{t^2+\theta^2+\phi^2} \sim \int_0^\delta dr \frac{tr}{t^2+r^2} \sim -t \ln |t| . \tag{17}$$

From this derivation, one expects that the occurrence of isolated zeros in det M will result in critical points of logarithmic type for those values of z_c at which the zeros occur.†

It is also worth showing the result of first doing the integral over ϕ in (5). In terms of $v = e^{i\phi}$, the ϕ integral becomes a contour integral around the unit circle in the complex v plane. Poles occur at $v = 0$ and also at the zeros of det M. Often det M is a low-order polynomial in v, and the locations of the poles can be found explicitly. For example, for the K model one has a pole at $v = -2z \cos\theta$. However, for several models introduced in Section 2, det M is a fifth-order polynomical in v, and even higher-order polynomials should be expected for more complex models, so it is of value to analyse theoretically what may occur. By the calculus of residues, contributions to the v integral come only from those poles that are inside the unit circle. These poles move around in the complex v plane, both as a function of z and as a function of θ, and it is the crossing and touching of these poles to the unit circle that gives rise to the non-analytic critical thermodynamic behaviour.

Let us first illustrate how the movement of the poles in the complex plane give rise to logarithmic non-analyticity using the special case of the 4–8/1 model as a specific example. Rewrite (15) as

$$\det M = -v(2z^2 \cos\theta) + 1 + 4z^4 - v^{-1}(2z^2 \cos\theta) \tag{20}$$

$$= \frac{-(v-v_1)(v-v_2)\, 2z^2 \cos\theta}{v}$$

†There is, however, one caveat that should be added. Even when there is only one zero in det M, it is possible that the scaling form of det M may have a more general form, such as

$$\det M \sim t^{2k} + \theta^{2m} + \phi^{2n}. \tag{18}$$

If so, then it is an easy exercise to show, for $m = n$, that near the critical point

$$E/N \sim -t^{-1} |t|^{2k/m} \ln |t| , \tag{19}$$

where for a bounded energy one must have $2k > m$. For example, if $k = \frac{3}{4}m$ then one would have $E/N \sim -t|t|^{-1/2} \ln |t|$, which would have a square-root divergence as the dominant specific-heat singularity. However, it is clear that this is not a K-type transition, and such a transition would be best thought of as a variation of the O-type transition. Such a variation could occur as a multicritical point in an extended phase diagram.

where $v = e^{i\phi}$ and where $v_{1,2}$ are the roots of the quadratic form. These roots are real and related by $v_1 = 1/v_2$. As the temperature approaches the critical point at $z = \sqrt{\frac{1}{2}}$, both poles approach 1, as θ approaches 0. The pole inside the unit circle has a residue proportional to $v_1 - v_2)^{-1}$, which behaves as $(t^2+\theta^2)-1/2$. The singular part of the energy then behaves as

$$\frac{E}{N} \sim \int_0^{\delta} \frac{t\,d\theta}{(t^2+\theta^2)^{1/2}} \sim -t \ln |t|\,, \tag{21}$$

as was previously found in (17).

A very different pattern of pole movement occurs in models that have K-type transitions. Using the K model as an example, one sees from (10) that for $z > \frac{1}{2}$ the pole in the complex ν plane at $-2z \cos\theta$ crosses from outside to inside the unit circle as θ increases from 0 to Θ given by (7). This means that the integral over θ in (6) of the residue of this pole has limits of $\pm\Theta$ and $\pi \pm \Theta$ for $z > \frac{1}{2}$ instead of the limits $\pm\pi$ for $z < \frac{1}{2}$. For all models known to the authors the integrand of this integral over θ is non-singular, and all the singular behaviour comes about from the thermal variation of the limit Θ, which behaves near the critical point as

$$\Theta \sim (z - z_c)^{1/2} \sim t^{1/2}. \tag{22}$$

Thus the singular part of E/N goes as $t^{1/2}$, above the transition only, and the specific heat diverges as $t^{-1/2}$.

The preceding analyses of the zeros of det $\boldsymbol{M}$ clearly show that there are two (at least) distinct kinds of singularities that should be expected for solutions of dimer models. There may be an isolated zero at z_c in det $\boldsymbol{M}$, and then in the second integral over θ in (5) two poles approach the unit circle, and each other, at one isolated value of z and θ. In this case one expects a symmetric logarithmic singularity and an O-type transition. In contrast, det $\boldsymbol{M}$ may have a pair of zeros for a range of z values, no zeros for a contiguous range of z values, and the pair of zeros merges at values z_c on the boundary between the two ranges. In this case, in the second integral over θ a pole crosses the unit circle continuously as a function of θ at a value of $\Theta(z)$, and at z_c the crossing ceases, i.e. $\Theta(z)$ approaches 0 or π. This behaviour leads to a K-type transition at z_c. It may further be noted that it is possible for the same model to have both kinds of transition because there may be many poles, some of which exhibit one kind of behaviour and others which exhibit the other kind.

While obtaining the exact solution for other models is not generally as easy as for the K model, for which the integrals can be expressed in

terms of simple functions, the preceding analysis allows one to diagnose whether the transition is K-type or O-type, and numerically accurate values for thermodynamic quantities are readily obtained from the integrals in (5). Using this analysis, a number of exact results are tabulated for a variety of dimer models in Section 5.

5 Results for thermodynamic properties

In this section basic exact results for the partition functions of a variety of dimer models are presented in a uniform way. The first result reported for each model is det $\boldsymbol{M}$ that appears in (2) or det $\boldsymbol{M}_1$ in (3). These determinants will generally be functions of several activities z_i, w_j and x_k, which will correspond to energies ε_i, δ_j and ξ_k. The determinants will also be functions of cos θ and $v = e^{i\phi}$, where θ and ϕ are the angles of integration in (2). The specific way of writing det $\boldsymbol{M}$ depends upon some trivial conventions. For example, since the integrals in (2) are over 2π, θ and ϕ can be replaced by their negatives or by their values incremented by constant values or by linearly independent combinations of θ and ϕ; these unimportant variations occur when the unit cell is chosen differently. The second result for each model is the location of the critical singularities in the (θ,ϕ) plane and the values of the activities at which the model has a transition. We shall only consider cases for which the ground-state energy is zero and all bond energies are either 0 or positive, so each critical value of the activities will lie in the interval [0,1]. The third result is whether the phase transition is of K-type or O-type, based on the analysis in Section 4.

5.1 VH family

Unit cells for some members of the VH family are shown in Fig. 2.3. The numbering pattern of the lattice sites that we found useful is specifically illustrated in Fig. 2.2 for the V^2H^2 model. It might be noted that the unit cells are in a rectangular pattern if the sum p of exponents on the V is even (e.g. V^2H^4 or $V^3H^2VH^2$) and in a triangular pattern if the sum p is odd (e.g. VH^4).

V model—same as K model

$$\det \boldsymbol{M}_1 = v^2 + v2z \cos \theta$$

The critical singularities occur at $(0,\pi)$ and $(\pi,0)$ for the critical value of the activity $z_c = \frac{1}{2}$. There is a K-type transition at $kT_c/\varepsilon = (\ln 2)^{-1} = 1.4426\ldots$.

V^4H^2 model

$$\det \boldsymbol{M}_1 = -v^3z^2 + v^2(3z^4+2z^3+1) - v(z^6+4z^5+z^4+3z^2) + z^6-2z^5\cos\theta + z^4$$

The critical singularities occur at $(0,0)$ for $z_c = 3^{-1/2}$. There is a K-type transition at $kT_c/\varepsilon = 1.8204\ldots$.

V^3H^2 model

$$\det \boldsymbol{M}_1 = v^6z^2 - v^4(2z^4+2z^3+1) + v^2(2z^5+z^4+2z^2) + 2vz^4\cos\theta$$

The critical singularities occur at $(0,0)$ and (π,π) for $z_c = \frac{1}{2}(5^{1/2}-1)$. There is a K-type transition at $kT_c/\varepsilon = 2.0780\ldots$.

V^2H^2 model

$$\det \boldsymbol{M}_1 = v^2z^2 - v(z^4+2z^3+1) + z^4-2z^3\cos\theta + z^2$$

The critical singularities occur at (π,π) for $z_c = 2^{-1/2}$. There is a K-type transition at $kT_c/\varepsilon = 2.8853\ldots$.

$V^3H^2VH^2$ model

$$\det \boldsymbol{M}_1 = v^4z^4 - v^32z^2(z+1)(z^3+z^2-z+1) + v^2(z+1)(6z^6-z^5+z^4+3z^3+z^2-z+1) - v2z^2(z+1)^2(z^2-z+1)(2z^2-z+1) + 2z^6(1-\cos\theta)$$

The critical singularities occur at $(0,0)$ for $z_c = 0.6738\ldots$. There is a K-type transition at $kT_c/\varepsilon = 2.5331\ldots$.

VH^2 model

$$\det \boldsymbol{M}_1 = -v^2z^2 + (2z^3+1) - v^{-1}2z^2\cos\theta$$

The only critical singularity occurs at (0,0) and (π,π) for $z_c = 1$ corresponding to $kT = \infty$.

V^2H^4 model

$$\det \boldsymbol{M}_1 = -v^3z^4 + v^2(z^6+2z^5+z^4+2z^2)$$
$$-v(2z^6+2z^5+2z^4+2z^3+1) + z^6-2z^4\cos\theta + z^2$$

The only critical singularity occurs at $(\pi,0)$ for $z_c = 1$ corresponding to $kT = \infty$.

V^2H^6 model

$$\det \boldsymbol{M}_1 = v^4z^6 - v^3(z^8+2z^7+2z^6+3z^4) + v^2(3z^8+4z^7+4z^6+4z^5+2z^4+3z^2)$$
$$-v(3z^8+2z^7+3z^6+2z^5+3z^4+2z^3+1) + z^8-2z^5\cos\theta + z^2$$

The critical singularities occur at $(\pi,0)$ for $z_c = 2^{-1/2}$. There is a K-type transition at $kT_c/\varepsilon = 2.88539\ldots$.

VH^4 model

$$\det \boldsymbol{M}_1 = v^6z^4 - v^4(2z^5+z^4+2z^2) + v^2(2z^5+2z^3+1) + v2z^3\cos\theta$$

The critical singularities occur at $(0,\pi)$ and $(\pi,0)$ for $z_c = 2^{-1/2}$. There is a K-type transition at $kT_c/\varepsilon = 2.88539\ldots$.

H^2 model

$$\det \boldsymbol{M}_1 = -vz^2 + z^2 + 2z\cos\theta + 1$$

The critical singularities occur at $(\pi,0)$ for $z_c = \frac{1}{2}$. There is a K-type transition at $kT_c/\varepsilon = 1.4426\ldots$.

There are some obvious systematic trends in the form of det $\boldsymbol{M}_1$ in the previous results. For models with a rectangular packing pattern for the unit cells (p even) det $\boldsymbol{M}_1$ is a polynomial in v of order $\frac{1}{2}(p+q)$, where $p+q$ is the sum of the exponents in the V^pH^q notation. For models with a triangular packing pattern (p odd) det $\boldsymbol{M}_1$ is a product of (a) v to some power and (b) a polynomial in v of order $p+q$ with all even powers missing except for the v^0 term. Clearly, for the general VH model det $\boldsymbol{M}_1$ may be of quite high order so that there are many poles to be considered

in (5). To find the zeros of det M_1, a simple computer program was written to scan the (z,θ,ϕ) space and to converge to the zeros. For the VH models there are no zeros for $z<z_c$, and at z_c a zero appears at $\theta=0$ for π. For $z>z_c$ this zero splits into two zeros at values of $\pm\Theta$, which for the case of the K model are given by (7). Except for the $V^3H^2VH^2$ model, the numerical values found for z_c suggested simple algebraic numbers, which were then verified algebraically and are listed in the results above.

For models in the VH family the temperature T_K at which the K-type transition occurs shows a general trend with ϱ_{vg}, the density of dimers on the vertical bonds in the ground state at temperature $T=0$. As seen in Fig. 5.1, T_K generally increases as ϱ_{vg} approaches $\frac{1}{3}$ from either side. This correlation is not perfectly smooth: indeed, two models with different values of ϱ_{vg} have the same values of T_K, and two models with the same value of ϱ_{vg} have different values of T_K. Nevertheless, the trend is apparent and is intuitively reasonable by considering the process of overturning a string of dimers from top to bottom on the lattice. We have been able to convince ourselves—on the basis of doodling with large copies of brick-lattice graph paper—that, compared with the K model, models with ϱ_{vg} closer to $\frac{1}{3}$ require more energy and gain less entropy per row, on average, to create such a string. However, we have not succeeded in making this into a quantitative argument to locate T_K except for the K (i.e. the V) model.

The VH^2 and the V^2H^4 models are clearly special in that they do not have K-type transitions or any other transition at all for finite temperatures.

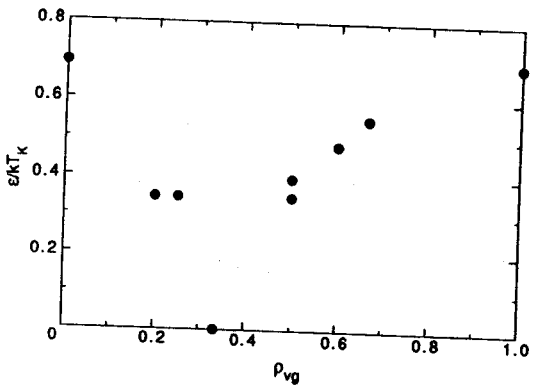

Fig. 5.1 The dimensionless inverse transition temperature, ε/kT_K versus density of vertical dimers in the ground state, ϱ_{vg}, for the VH models solved in this review.

Considering only Fig. 5.1, one might suggest that for all finite temperatures these two models are in ordered phases corresponding to the low-temperature ordered phases existing in the other models. This view is supported by the fact that there are no zeros in $\det \boldsymbol{M}(z,\theta,\phi)$, just as there are no zeros in the ordered low-temperature phases for the other VH models, in contrast with their high-temperature phases above T_K. On the other hand, there is good reason to suggest that these models are in disordered phases, like the high-temperature disordered phases in the other VH models. As T increases to ∞ in the other models, ϱ_v approaches $\frac{1}{3}$, whereas ϱ_v is already $\frac{1}{3}$ at $T=0$ for the VH^2 and V^2H^4 models and remains at $\frac{1}{3}$ for all higher temperatures. This means that these two models do not require overturning strings of dimers from top to bottom of the lattice in order to achieve the completely disordered $T=\infty$ state, consistent with these models being effectively disordered for any non-zero T.

VH^2/V model

An additional perspective on the question in the preceding paragraph is obtained from the solution of the VH^2/V model. The VH^2/V model was defined in Section 2 as having an energy ε for dimers on those bonds that are high-energy bonds for the V model (i.e. the vertical bonds) *plus* an energy δ for dimers on those bonds that are high-energy bonds for the VH^2 model. With activities $z = e^{-\varepsilon/kT}$ and $w = e^{-\delta/kT}$, dimers on some bonds of the model have activities z or w or zw or 1. For this model

$$\det \boldsymbol{M}_1 = -v^2w^2 + z^2(2z^3+1) - v^{-1}2w^2z^3\cos\theta\,.$$

A critical singularity of K type occurs at (0,0) on the line $w=z$. Another critical singularity of K type occurs at $(\pi,0)$ on the line $2z^2w^2-w+z=0$. The result is the phase diagram shown in Fig. 5.2(a). For $\varepsilon > \delta$ and for low temperatures the VH^2/V model remains completely frozen into the same phase as the K model with all vertical dimers, $\varrho_v=1$, and then at higher temperatures it undergoes a K-type transition to a phase with varying ϱ_v and varying density of domain walls (the phase labelled IC in Fig. 5.2a). In contrast, for $\delta > \varepsilon$ the model has no phase transition and resides exclusively in a single phase, which is characterized by $\varrho_v = \frac{1}{3}$ but which is *not* rigidly ordered. From the perspective of Fig. 5.2(a), it is clear that this phase is distinct from either the low- or the high-temperature phases of the K (i.e. V) model.

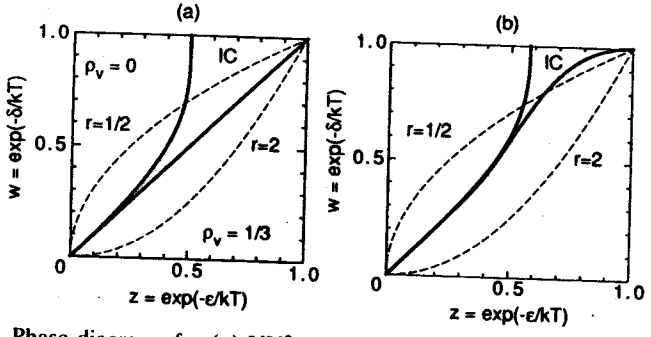

Fig. 5.2 Phase diagrams for (a) VH^2/V model and (b) VH^2/V^4H^2 model. Loci of transitions (two bold lines) and two representative physical trajectories (two dashed lines for $r = \delta/\varepsilon = 2$ and $\frac{1}{2}$).

VH^2/V^4H^2 model

As a function of temperature, the VH^2/V model is not very interesting because it behaves in the same way as the V model for $\varepsilon > \delta$ and in the same way as the VH^2 model for $\varepsilon < \delta$. More interesting in this regard is the VH^2/V^4H^2 model. For this model

$$\det \boldsymbol{M}_1 = -v^3z^2w^4 + v^2[2z^3w^5(z+1)+w^2(z^4+1)] - v[z^4w^6(z+1)^2+2z^2w^3(z^3+1)+z^2] + z^4w^4(z^2-2z\cos\theta+1)$$

The critical singularities occur at (0,0) and $(\pi,0)$ in the (θ,ϕ) plane. The loci of the transitions are shown in Fig. 5.2(b). Topologically, the arrangement of this phase diagram in Fig. 5.2(b) is the same as that in Fig. 5.2(a). However, as a function of temperature the VH^2/V^4H^2 model undergoes two transitions when $\varepsilon > \delta$, as can be seen from the $r = \frac{1}{2}$ line in Fig. 5.2(b). From this perspective, the phases in the lower right-hand sides of Figs. 5.2(a) and (b) would appear to be best characterized as high-temperature disordered phases, at least relative to the other two phases in these phase diagrams.

5.2 Models based on the 4–8 lattice

The 4–8 lattice family of dimer models is very rich and has yet to be fully and systematically mapped. Therefore the list of models chosen for this review should be looked upon as an exploration, rather than a complete

and systematic classification. However, there is one fairly obvious classification principle that we have followed. This is to classify the models by the size of the unit cell. Since the smallest unit cell consistent with the 4–8 lattice (see Fig. 2.6) is a square, and larger unit cells consist of integer numbers p of squares, our classification scheme consists of naming the models 4–8/p/i, where i is an arbitrary integer that distinguishes different models with the same p value. Unit cells for the following models are shown in Figs. 2.6–8. The specific numbering of sites that we found useful is illustrated in Fig. 2.7(b) for the 4–8/2/2 model.

4–8/1 model

The 4–8/1 model shown in Fig. 2.6 is the general case for models on the 4–8 lattice with unit cell containing only one basic square, i.e., four lattice sites. It may be noted that the matrix $\boldsymbol{M}$ does not decompose into two off-diagonal $\boldsymbol{M}_1$ blocks. For this model

$$\det \boldsymbol{M} = -vx_1x_2(z_1z_2e^{i\theta}+z_3z_4e^{-i\theta}) + (z_1z_2+z_3z_4)^2 + (x_1x_2)^2 - v^{-1}x_1x_2(z_1z_2e^{-i\theta} + z_3z_4e^{i\theta}) .$$

The critical singularities occur at (0,0) for $z_1z_2 + z_3z_4 = x_1x_2$. These singularities yield lines of O-type transitions.

A simple special case of the 4–8/1 model is the SCD model (Salinas and Nagle, 1974), for which $x_1 = x_2 = 1$ and $z_1 = z_2 = z_3 = z_4$. Then

$$\det \boldsymbol{M} = -v2z^2\cos\theta + 4z^4+1 - v^{-1}2z^2\cos\theta ,$$

and the critical singularities occur at (0,0) for $2z^2 = 1$, yielding an O-type transition at $kT_c/\varepsilon = 2.8853\ldots$.

4–8/2 models

The result that there are only O-type transitions for the 4–8/1 model is not a good indicator of the rich variety of results for larger p, to which we now turn. The three models in the 4–8/2 class all have the property of being "staggered" models in the sense that there are two types of squares, A and B, and each square is completely surrounded by squares of the other type as shown in Fig. 3.1. It may also be useful to note that the angle θ, not ϕ, corresponds to the vertical direction in Fig. 2.7.

4–8/2/1 model

$$\det \boldsymbol{M}_1 = -v2w^2\cos\theta + 4z^2w^2+1 - v^{-1}2z^2\cos\theta$$

The critical singularities occur at (0,0) and (π,π) for $z_c = 2^{-1/2}$ *and* for $w_c = 2^{-1/2}$. The loci of the critical singularities are shown as bold lines in the (w,z) plane in Fig. 5.3(a); these lines divide the (w,z) plane into four regions, which will be called the low-temperature region (LT), the high-temperature region (HT), and two intermediate-temperature regions, denoted IT+ and IT− in Fig. 5.3(a). Also shown by dashed lines in this figure are three loci for physical values of (w,z) as a function of temperature for three different values of the ratio $r = \delta/\varepsilon$ of the two energies in the model.

In the general case ($r \neq 1$), as T increases from zero, the physical locus of (w,z) crosses one of the bold lines in Fig. 5.3(a) and there is a K-type transition at T_{K1}, as shown in Fig. 5.3(b). As T increases further to T_{K2}, (w,z) crosses the other bold line. This is accompanied by a square-root divergence in the specific heat as this second transition is approached from below, as shown in Fig. 5.3(b), and analytic behaviour of the specific heat above this second transition. This behaviour will be called an inverted K-type transition. In the limit when δ/ε goes to infinity there is only one K-type transition. When δ/ε goes to zero there is one inverted K-type transition. For the special case $\varepsilon = \delta$ ($r=1$) the 4–8/2/1 model reduces to a 4–8/1 model and has a single O-type transition, which therefore appears as a multicritical point in the larger 4–8/2/1 phase diagram in Fig. 5.3(a). In this context, the crossover from the "typical" behaviour of two K-type

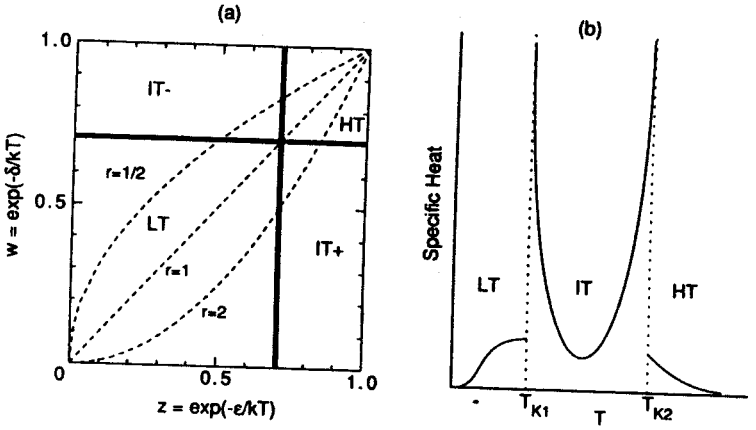

Fig. 5.3 4–8/2/1 model. (a) Loci of transitions (bold lines) and physical trajectories (dashes lines) in the (w,z) plane for $r = \delta/\varepsilon = 2$, 1 and $\frac{1}{2}$. (b) Specific heat verus temperature for the general case $r \neq 1$.

transitions to the O-type multicritical point has been fully described (Nagle and Yokoi, 1987) and carries a crossover exponent $\phi=1$.

The domain-wall isomorphism leads to physical insight into the exact thermal behaviour of the 4–8/2/1 model. These domain walls are illustrated in Fig. 3.1. The density of walls of z type minus the density of walls of w type equals the density of dimers of z type minus the density of dimers of w type, which we shall call ϱ_{z-w}. The exact solution shows that ϱ_{z-w} is zero in the low-temperature LT phase and in the high-temperature HT phase of the 4–8/2/1 model. In the IT± phases between the two K-type transitions ϱ_{z-w} is non-zero. This is a powerful result when coupled with some simple observations about the domain walls. Localized excitations contribute nothing to ϱ_{z-w}. The only way to obtain $\varrho_{z-w} \neq 0$ is to have some walls that run from top to bottom of the lattice (with reversals permitted) and with an excess of one wall type over the other. (The example in Fig. 3.1 has $\varrho_{z-w} = -\frac{1}{6}$.) A non-zero value of ϱ_{z-w} is the intuitive characterization of the intermediate phase of the 4–8/2/1 model. The low-temperature phase certainly has localized excitations. It has not been shown whether or not the LT phase has a non-zero but equal density of extended domain walls of z type and w type, but the authors speculate that the density of both wall types is zero in this phase. The high-temperature phase probably has many extended domain walls as well as localized excitations. It is not clear whether the HT phase is a completely disordered phase or whether some residual order extends to $T=\infty$.

By far the most interesting of the three 4–8/2 models is the 4–8/2/1 model. The other two models are presented for contrast to show how apparently small variations in the models leads to large and qualitative variations in the thermal behaviour.

4–8/2/2 model

$$\det \boldsymbol{M}_1 = -v2zw\cos\theta + 4z^2w^2 + 1 - v^{-1}2zw\cos\theta$$

The critical singularities occur at (0,0) and (π,π) for $zw = \frac{1}{2}$. This yields a line of O-type transitions in the (w,z) plane. For any fixed values of the energies ε and δ the 4–8/2/2 model has a simple O-type transition.

4–8/2/3 model

$$\det \boldsymbol{M}_1 = -v^2 2zw\cos\theta + (z^2 + w^2)^2 + 1 - v^{-1}2zw\cos\theta$$

The critical singularities occur at (0,0) and (π,π) only for $z_c = 2^{-1/2} = w_c$, at which there is an O-type transition. Therefore the 4–8/2/3 model

has no transition at all, except when $\varepsilon = \delta$, in which case it is a special case of the 4–8/1 model.

4–8s/2/1 model

The 4–8s/2/1 model involves a modification of the 4–8 lattice. While our classification scheme would suggest that this modification might occur elsewhere in the list, the domain-wall isomorphism compels discussion of it with the 4–8/2/1 model. In the domain-wall picture this model has an extra degree of freedom, which consists of allowing domain walls to annihilate with walls of the same type, as well as with walls of opposite type as in the 4–8/2/1 model. With this modification, the $\boldsymbol{M}$ matrix does not decompose into two off-diagonal $\boldsymbol{M}_1$ blocks. For this model

$$\det \boldsymbol{M} = (v^2 + v^{-2})4z^2w^2(\cos^2\theta - x^2) - (v + v^{-1})2(z^2+w^2)$$
$$(4z^2w^2+1-x^2)\cos\theta + (4z^2w^2+1)^2$$
$$+ 4(z^4+w^4)\cos^2\theta + x^4 - 2x^2\cos 2\theta .$$

The critical singularities occur at (0,0) and (π,π) for $(2z^2-1)(2w^2-1) = x^2$. This gives two non-intersecting lines in the (w,z) plane; an example is given in Fig. 3 of the paper by Nagle and Yokoi (1987). For fixed energies ε, δ the (w,z) trajectories cross each of these lines, so there are two transitions, each of which is O-type. In this context, the K-type transitions in the 4–8/2/1 model are multicritical points at $\xi = 0$ in the 4–8s/2/1 model.

3–12/1 model

The 4–8s/2/1 model reduces to the 3–12/1 model when $\delta = \infty$ $(w=0)$. In this case the multicritical point is the single K-type transition of the K model, for which there is only one type of domain wall. This was first discovered by Bhattacharjee (1984), who also calculated that the conventional crossover exponent is $\phi = \frac{1}{2}$.

4–8/4 models

Stimulated by the interesting thermal behaviour that appears when models are considered on the 4–8 lattice with unit cells having more than $p=1$ square, we have begun exploration of models with $p=4$ squares.

4–8/4/1 model

$$\det \boldsymbol{M}_1 = (v^2 + v^{-2})z^2w^2 - v(8z^3w^3+z^2+w^2) - v^{-1}[4z^2w^2(z^2+w^2)+2zw] + (4z^3w+1)(4zw^3+1) - 2z^2w^2\cos\theta$$

When the bond energies ε and δ for the z and w bonds respectively are greater than zero, the critical singularities occur at (0,0) for $2zw = 1$, at which there is a line of O-type transitions. Additionally, when either ε or δ is less than zero, this model has several phase transitions of both K type and O type. The details of these transitions will be given in a subsequent publication.

4–8/4/2 model

By way of contrast, we also list the 4–8/4/2 model. It has the same underlying motif as the 4–8/4/1 model in that the four squares in the unit cell are related by $\frac{1}{2}\pi$ rotations. Nevertheless, the 4–8/4/2 model has no transition except in the limit $\varepsilon = \delta$, in which case it reduces to a 4–8/1 model. For the 4–8/4/2 model

$$\det \boldsymbol{M}_1 = (v + v^{-1})zw(z^2-2zw\cos\theta + w^2) + 16z^4w^4+(z^2+w^2)^2+1+2zw(z^2+w^2)\cos\theta .$$

The critical singularities occur at (π,π) only for $z_c = w_c = 2^{-1/2}$, at which there is an O-type transition.

5.3 Other models

Staggered quadratic lattice model

The SQK model is shown in Fig. 2.4. For this model

$$\det \boldsymbol{M}_1 = -v + 2w+2z^2(1-\cos\theta) - v^{-1}w^2.$$

The critical singularities occur at $(\pi,0)$ for $1 - 2z_c = w_c$ and there is a line of K-type transitions. In the case when $w > 1$ the phase boundary is $1 + 2z_c = w_c$, and the low-temperature ordered phase has all the w-bonds filled with dimers. The point $w = 1$, $z = 0$ corresponds to the square-lattice model, which has no phase transition and which appears as a multicritical point in the phase diagram for the SQK model. It may also be worth noting, in passing, that these two low-temperature phases are similar to the valence-bond crystals discussed in connection with the resonating valence-bond theory of high-T_c superconductors (Rokhsar and Kivelson, 1988).

6 Correlation functions

While determination of the thermodynamic functions at phase transitions is one of the main goals of solving models, it is clearly established that the determination of the correlation functions leads to considerably enhanced insight. In the case of the two-dimensional Ising model the correlation functions decay exponentially with distance as $e^{-r/\xi}$, where the correlation length ξ increases as the critical point is approached according to $\xi \sim t^{-\nu}$. Right at the critical point the correlations decay only algebraically as $r^{-d+2-\eta}$, where $\eta = \frac{1}{4}$ in two dimensions. As the correlations become longer-range near the critical point, the lattice structure becomes less important and the long-range correlations become isotropic in direction on the lattice (Hartwig and Stephenson, 1968). This leads to an essential characterization of the critical point in the Ising model and many other spin-type models, namely that it is a state of the system in which all spins are well correlated in an isotropic fashion. As we shall see, the correlation functions for models with K-type transitions present a strongly contrasting picture to this standard picture developed for spin-type systems.

Fortunately, the method for computing correlation functions for two-dimensional dimer models has been well established by Fisher and Stephenson (1963). Unfortunately, carrying out the method in the detail necessary to obtain reliable results involves a great deal of tedious calculation. This accounts for the fact that results for the correlation functions for models with K-type transitions are known only for the simple K model and not for any of the other interesting models discussed in the previous sections. Nevertheless, the results for the K model already yield much essential insight into K-type transitions.

The dimer pair-correlation function $C_{ab}(x,y)$ is defined as

$$C_{ab}(x,y) = P_{ab}(x,y) - P_a P_b, \tag{23}$$

where P_a and P_b are the probabilities that bond types a and b respectively are occupied by dimers, and $P_{ab}(x,y)$ is the joint probability that both bond a located at the origin (0,0) and bond b located at (x,y) are occupied by dimers. Using the perturbation theory of Pfaffians, C_{ab} can be expressed in terms of Green's functions, which typically look like

$$G(x,y) = \int_0^{2\pi} d\theta \int_0^{2\pi} d\phi \frac{e^{-ix\theta - iy\phi}}{|z - ze^{i\theta}|^2 - e^{-i\phi}}. \tag{24}$$

The integration over ϕ may be performed analytically and the remaining integration over θ may be evaluated numerically to produce tables of correlation functions for varying x and y. More elegantly, the asymptotic

expressions for the Green's functions at long distances and for temperatures close to T_K have been obtained. Since the ensuing asymptotic or scaling form of the correlations functions reveals most of the significant physical features, this review will focus upon these only, although the original paper (Yokoi *et al.*, 1986) shows some of the numerical results for one specific temperature. Furthermore, the functional forms of these scaling functions are essentially the same, regardless of the two bond types involved; the differences are contained in fairly simple factors whose temperature dependence is modest and with a minus sign when one of the dimers is vertical and one is horizontal.

The first striking feature of the asymptotic form of the scaling functions is that they depend upon two scaling lengths ξ_x and ξ_y, which are naturally identified as the correlation lengths in the x and y directions respectively because of the way they appear in the formula for the correlation functions given by

$$C_{ab}(x,y) \sim \frac{(x/\xi_x)^2 \sin^2(x/\xi_x) - (y/\xi_y)^2 \cos^2(x/\xi_x)}{\xi_x^2[(x/\xi_x)^2 + (y/\xi_y)^2]^2}. \tag{25}$$

The divergence of the two correlation lengths is quite different as a function of reduced temperature t as the K-type transition is approached from above, with

$$\xi_x \sim t^{-1/2}, \qquad \xi_y \sim t^{-1}. \tag{26}$$

The existence of two independent and functionally disparate correlation lengths requires the use of two critical exponents ν_x and ν_y to describe the divergence of the correlation lengths, ν_x in the x direction and ν_y in the y direction. Equation (26) shows that the numerical value of ν_x is $\frac{1}{2}$ and the numerical value of ν_y is 1. The fact that two critical exponents are required to describe the critical correlation behaviour is a major indicator of the essential anisotropy of the K model. The values of these critical exponents agrees with the values obtained by Schultz (1980) in connection with commensurate–incommensurate transitions, and they obey the anisotropic hyperscaling relation (Fisher, 1986)

$$\nu_x + \nu_y = 2 - \alpha. \tag{27}$$

Another major indicator of the essential anisotropy in the model is the spatial pattern of the correlation functions. This is emphasized in Fig. 6.1, which shows the pattern of positive and negative values for correlation functions for a horizontal dimer located anywhere, given that there is a horizontal dimer at the origin. Since domain walls pass through the horizontal dimers, this is essentially the domain-wall/domain-wall

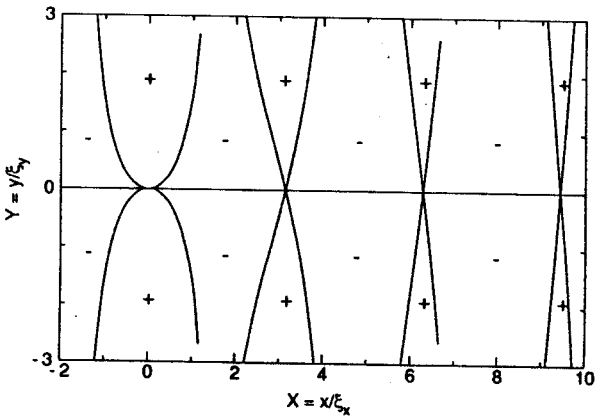

Fig. 6.1 The pattern of positive and negative regions for the domain-wall/domain-wall correlation function in the asymptotic scaling limit. The X and Y axes are the actual distances x and y scaled by the correlation lengths in the respective directions.

correlation function. Because of the anisotropic forcing constraint, a wall at the origin gives rise to positive correlations for finding a wall near $x = 0$ for non-zero values of y. In addition, there are positive correlations for finding walls at regular spacings along the x axis, corresponding in an obvious way to the bulk density of walls. Because the walls repel each other, the correlation function is negative in-between.

Another important feature to appreciate, which was first published by Sutherland (1968), is that the correlation functions fall off with distance only as r^{-2}, even when the temperature is greater than the transition temperature T_K. This is in strong contrast with the models with O-type transitions, such as the Ising model (McCoy and Wu, 1973) or the 4–8/1 dimer model (Salinas and Nagle, 1974), for which the correlation functions decay exponentially as $e^{-r/\xi}$ when $t \neq 0$ and only decay algebraically right at the critical point.

7 Finite-size effects

There has been a long-standing interest in how phase transitions develop as system sizes become infinite. Experimentally, this interest arises naturally because real samples have finite sizes. Theoretically, it is impossible for the partition function of a finite system to behave non-analytically, so it is natural to enquire how smooth analytic functions can

develop singularities. Consequently, there has been a good deal of work performed on exactly solvable models, such as the Ising model. To put the analytical results into a form that can be extended to models not solved or to real systems, the finite-size scaling theory has been developed to represent models in the critical region, as has been reviewed by Barber (1983).

It is appropriate to ask whether finite-size scaling theory pertains to models with K-type transitions, for which one can, with some effort, obtain complete results for finite as well as infinite systems. As was the case for the correlation functions discussed in Section 6, explicit calculations have only been performed for the K model and not for the other models that exhibit K-type or inverted K-type transitions. It turns out that the K model does obey finite-size scaling provided that the theory is suitably extended. This extension requires an extra variable to account for a shape dependence. In terms of the correlation functions discussed in Section 6, this shape dependence stems from the anisotropy in the correlation lengths in the two directions. The exact asymptotic scaling function depends dramatically upon this shape variable, ranging from a smooth function for one limiting shape to a sequence of delta functions for another limiting shape.

Figure 7.1 shows the specific heat for the K model for a brick lattice with $M = 20$, 40 and ∞ rows in the vertical direction and $N = \infty$ rows in the horizontal direction. The buildup of the specific-heat peak at T_K with increasing M appears reasonable, with the asymmetrical character of the bulk ($M = \infty$) result appearing already. Unlike the Ising model, however, where the specific heat approaches its bulk value at a fixed non-critical temperature exponentially (e^{-M}), the approach for the K model is algebraic (M^{-2}) for $T > T_K$ (Bhattacharjee and Nagle, 1985). This is consistent with the algebraic decay of the correlations for $T > T_K$ discussed in Section 6.

In striking contrast with the behaviour described in the preceding paragraph, the specific heat for the K model on a brick lattice with $M = \infty$ rows and $N =$ finite columns consists of a sequence of delta functions. The first delta function occurs at T_K and corresponds to the formation, as temperature is increased, of the first domain wall. The second delta function occurs at a higher temperature given by $2\cos^2(\pi/2N) = e^{\varepsilon/kT_2}$ and corresponds to the formation of a second domain wall. Between T_K and T_2, the system remains frozen into the state with precisely one domain wall, and the specific heat is zero. For finite N subsequent delta functions appear at higher temperatures, T_n, and the thermodynamic state of the system develops an nth wall. The integrated (over T) strength

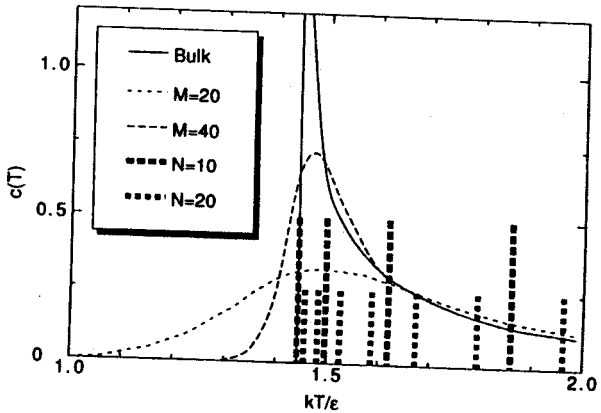

Fig. 7.1 Specific heat per lattice site versus temperature for two short fat lattices of size $20 \times \infty$ and $40 \times \infty$, two tall thin lattices of size $\infty \times 10$, $\infty \times 20$ and the bulk system of size $\infty \times \infty$.

of each delta function corresponds to the energy required to create one additional domain wall. As N becomes larger, the delta functions become denser, but with smaller integrated strength proportional to ε/N for the specific heat per lattice site. The density of delta functions approaches infinity at all temperatures, but at T_K the approach is more rapid than $1/N$, so that the bulk thermodynamic limit consisting of the $t^{-1/2}$ divergence in the specific heat is recovered.

The contrast in behaviour between the two shapes for the K model discussed in the preceding two paragraphs indicates that any finite-size scaling theory must have a scaling function that is strongly shape-dependent as well as being dependent upon the reduced temperature t. After a laborious analysis of cases, the following form was found to do the job. The asymptotic scaling form for specific heat per lattice site, $c_{N\times M}(t)$, for a lattice with M rows and N columns may be written as

$$c_{N\times M}(t) = k\mathcal{M}^{1/2}\mathcal{P}(\tau, r), \tag{28}$$

where

$$\mathcal{M} = \frac{MN^2}{M+N^2}, \quad \tau = \mathcal{M}t, \quad r = \frac{N^2}{M},$$

and the function $\mathcal{P}$ is the finite-size scaling function.

It is illuminating to compare (28) with the usual finite-size scaling form for isotropic systems, which is usually written as

$$c_{M\times M}(t) = kM^{\alpha/\nu}\mathcal{P}(tM^{1/\nu}). \tag{29}$$

The prefactor $\mathcal{M}^{1/2}$ in (28) has two limiting cases that should be compared to the prefactor $M^{\alpha/\nu}$ in (29). In both limiting cases the divergence of the specific heat is given by $\alpha = \frac{1}{2}$. In the case when N^2 goes to ∞ faster than M, $\mathcal{M} \sim M$. Since the divergence of the correlations in the vertical direction has a critical exponent $\nu_y = 1$, the prefactor is consistent with the finite size-scaling form. In the case when M goes to ∞ faster than N^2, $\mathcal{M} \sim N^2$ and the prefactor is given by N^1, which is consistent with a critical exponent $\nu_x = \frac{1}{2}$ in N^{α/ν_x}. Similarly, the first scaling variable τ in the $\mathcal{P}$ function goes as tM or tN^2 in the two preceding cases. Again, by comparison to the form in (29), this requires the two critical exponents $\nu_x = \frac{1}{2}$ and $\nu_y = 1$. This much could have been predicted from the correlation-function results reviewed in Section 6. Actually, the finite-size-scaling results preceded the correlation-function results. When the finite-size-scaling results were determined, it was strongly suggested that the values of ν_x and ν_y were $\frac{1}{2}$ and 1 respectively. However, since that conclusion depended upon the assumption that the finite-size-scaling theory was correct, it was conservatively concluded (Bhattacharjee and Nagle, 1985) that there were two finite-size-scaling exponents ν_M and ν_N with those two values. Now that the correlation function calculations have been performed, there is no doubt that $\nu_N = \nu_x = \frac{1}{2}$ and $\nu_M = \nu_y = 1$ *and* that the suitable extended finite-size-scaling theory is correct.

In addition, it is clear that the scaling function $\mathcal{P}$ in (28) *also* depends dramatically upon a second anisotropic variable, $r = N^2/M$, which describes the relative dimensions of the finite lattice. To illustrate how dramatic this dependence is, Fig. 7.2 shows $\mathcal{P}$ as a function of τ for several values of r.

For the $M \times \infty$ lattices the $\mathcal{P}$ function is smooth with a maximum a little above $\tau = 0$. This means that the temperature at which the maximum in the specific heat occurs is greater than T_K for finite M, as seen in Fig. 7.1. The fact that $\mathcal{P}(\tau)$ goes to zero exponentially fast for $\tau < 0$ means, according to (28), that the specific heat at any fixed temperature below T_K (fixed negative t) goes to zero as M goes to ∞. Turning again to the general case of $N \times M$ lattices, as $r = N^2/M$ becomes less than ∞, $\mathcal{P}$ develops oscillations as a function of τ. As r is reduced below 1, these oscillations begin to develop into peaks, which, as r goes to 0, become the delta functions characteristic of the long thin $\infty \times N$ lattice.

The behaviour described in the preceding paragraph may be compared with the asymptotic behaviour of the specific heat of the two-dimensional Ising model (Ferdinand and Fisher, 1969), who, in addition to obtaining an exact form, gave the following convenient approximate from:

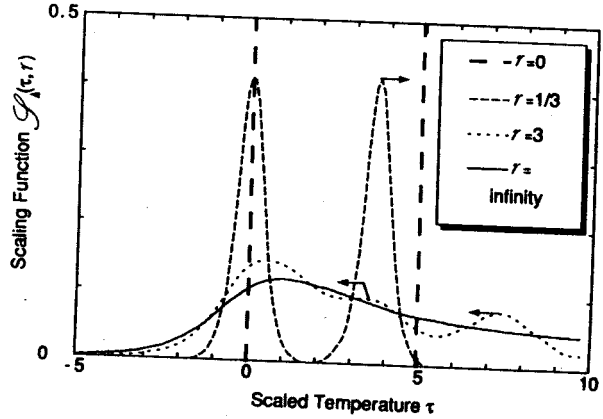

Fig. 7.2 The scaling function for the specific heat $\mathcal{P}$ as a function of the scaled temperature τ for several values of the anisotropy parameter r as indicated. The arrows on the peaks of the $r = \frac{1}{3}$ and $r = 3$ curves show the direction of their movement as r decreases.

$$\frac{C(T)}{kMN} \sim -\ln\left[\left(t + \frac{a^*}{N}\right)^2 + \left(\frac{b}{N}\right)^2\right], \tag{30}$$

where a^* depends upon the shape parameter $s = M/N$ and there is the obvious symmetry that $a^*(s) = a^*(1/s)$. In contrast, for the K model the scaling function is an essentially more complicated function of r, and there is no obvious symmetry in r.

8 Three-dimensional models

A natural question to ask is whether there are models in dimensions greater than two that have K-type transitions. Although there are no exact solutions† to answer this question rigorously, the answer is almost certainly that there are such models, provided that one allows for the critical exponent α to vary with dimension d. The simplest three-dimensional model has a lattice that is sketched in Fig. 8.1. This lattice bears the same relationship to the simple cubic lattice as the brick lattice bears to the square lattice, namely half the vertical bonds are removed in an alternating pattern in any direction. This lattice will be called the

†There is one exactly solved three-dimensional dimer model (Priezzhev, 1981), but it does not have a phase transition.

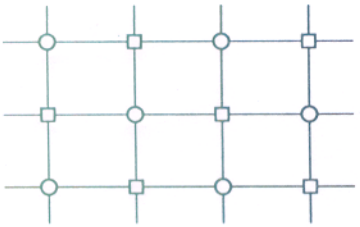

Fig. 8.1 A horizontal slice of the modified simple cubic lattice. The bonds in each horizontal plane form a square lattice as shown by the lines. Each lattice site has only one vertical bond connecting to one of the two neighbouring horizontal planes instead of two as for the unmodified simple cubic lattice. Those vertical bonds indicated by open circles on the lattice site are connected to the plane above the plane shown, and those vertical bonds indicated by open squares are connected to the plane below.

modified simple cubic lattice. As with the two-dimensional K model, the energy for dimers will be taken to be 0 if the dimer is on a vertical bond and ε if it is on a horizontal bond. We will call this model the 3-d K model. It was first discussed by Izuyama and Akutsu (1982a), who also discussed the three-dimensional analogue of the SQK model (Izuyama and Akutsu, 1982b).

The ground state of the 3-d K model has all the dimers on vertical bonds, and each vertical bond has a dimer. Let us consider perturbations from the ground state. Just as for the 2-d K model, moving any vertical dimer onto a horizontal bond causes a chain reaction of moves so that each plane in the lattice has a horizontal dimer. The only minor difference is that for the 3-d K model there are four options in each plane for making the move instead of two. By the same argument used for the 2-d K model, this locates $kT_K = \varepsilon/\ln 4$, and indicates that for $T < T_K$ the model is frozen into its ground state. Above T_K, each microstate of the system is characterized by a unique set of repelling dislocation lines connecting horizontal dimers in successive levels, thereby exhibiting the essential nature of the anisotropy in the model. Thus the assertion is justified that higher-dimensional models with K-type transitions exist,† although these observations do not determine the nature of any thermodynamic non-analyticity above T_K, nor would one expect α to remain $\frac{1}{2}$ for dimension higher than two.

†There is a different kind of extension of the 2-d K model that one could also imagine—one in which the microstates of the model would consist of repelling 2-d surfaces (not necessarily flat), each of which would stretch from top to bottom of the system, but this kind of model would not appear to arise from dimer models.

Although the 3-d K model has not been solved, it has been argued that $\alpha = 0$. The first argument was presented as an exact calculation by Izuyama and Akutsu (1982a); it gave a finite specific heat at T_K. This argument was shown to be in error by Bhattacharjee *et al.* (1983) and was shown to be similar to a Bethe approximation (Kornilov and Priezzhev, 1984). Bhattacharjee *et al.* (1983) agreed that $\alpha = 0$, but suggested that a logarithmic divergence of the specific heat above T_K is likely. They also suggested that the specific heat at T_K remains finite for d greater than 3. While the nuances of the discussion are best left to the primary papers, it is worth indicating the main features of the analysis.

The discussion is based on one rigorous calculation for finite systems, which yields complete details of the second perturbation from the ground state, namely those states involving two horizontal dimers in each plane. This might seem to be a weak base for any calculation of α if one thinks of spin systems in which many perturbations have already occurred before the transition takes place. The reason it is a useful base in the K models, both 2-d and 3-d, is that the models remain in their ground state up to T_K and the first perturbation already determines T_K, so additional low-lying excitations may also be informative. How this may be so is indicated in Fig. 7.1 by the calculation for 2-d lattices of size $\infty \times N$. For the 3-d model the comparable calculation will be for an infinite stack of finite planes of size N^2. For systems of this shape the specific heat consists of delta functions, as shown in Fig. 7.1, which become denser as the system size becomes larger. In the infinite limit the density of delta functions determines the value of the specific heat. The idea is to approximate this density of delta functions at T_K from the first two delta functions. The first of these delta functions corresponds to the system going from the ground state to states with one string of horizontal dimers, and the second delta function corresponds to the system going on to states with two strings of horizontal dimers. Although obtaining the details of the second delta function is a good deal more challenging than for the first delta function, it is a calculation that can be performed using random-walk techniques developed by Montroll (1969).

The result of the rigorous calculation and its non-rigorous extrapolation to the thermodynamic behaviour is best described in terms of the free energy per lattice site, $f(\varrho)$, as a function of the density of horizontal dimers, ϱ. For $d = 2$ the analysis yields

$$f(\varrho) \sim -t\varrho + b\varrho^3 + \text{higher-order terms}. \tag{31}$$

From (31) one obtains $\varrho^2 \sim t$ for small t. Since the energy $E = \varrho\varepsilon$, this yields a specific heat $C = \mathrm{d}E/\mathrm{d}t \sim t^{-1/2}$. The agreement with the exact result lends confidence in this analysis. For $d = 3$ the same analysis yields

$$f(\varrho) \sim -t\varrho - \frac{b\varrho^2}{\ln \varrho} + \text{higher-order terms} . \tag{32}$$

From (32) one obtains $\varrho \sim -t \ln t$, which yields a logarithmic divergence in the specific heat as t goes to zero at T_K. For $d > 3$

$$f(\varrho) \sim -t\varrho - b\varrho^2 + \text{higher-order terms} , \tag{33}$$

which yields a finite specific heat at T_K.

9 Application to biomembranes

The structure of biomembranes is determined by the lipid component, which forms lipid bilayers as shown in Figs. 9.1(a,b). The lipids portrayed in Fig. 9.1 are amphiphilic molecules of molecular weight *ca.* 600–1000, with headgroups containing charges that prefer an aqueous environment and with hydrocarbon tails that, like oils, phase-separate from water. These molecules have many internal (i.e. conformational) degrees of freedom. Especially important and most numerous are the conformational degrees of freedom of the hydrocarbon chains, which are basically $-(CH_2)_nCH_3$, where each $n \approx 12$–18. Each of the $(n-1)$ C—C bonds joining two methylene (CH_2) groups has a conformational, rotameric degree of freedom, which is conventionally modelled in polymer physical

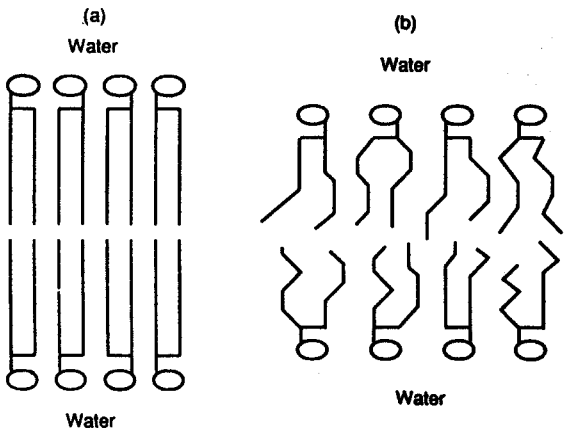

Fig. 9.1 Schematic sketches of small sections of lipid bilayers for (a) below the main transition and (b) above the main transition. Each bilayer section shows eight lipid molecules, with headgroups indicated by ovals and tails by solid lines.

chemistry by three states: one *trans* ground state and two *gauche* states with energies $\varepsilon \sim kT$ for biological temperatures. In Fig. 9.1(a) the hydrocarbon chains are pictured with all rotameric states *trans*. In Fig. 9.1(b) *gauche* states have been introduced.

Since lipid molecules have complex internal structure, it is not surprising that a description of their condensed-matter phases requires many different concepts of order/disorder. As with simple spherical atoms, there may be positional order/disorder. The symmetry of each lipid is so low that there may also be orientational order/disorder, which may be thought of as headgroup order/disorder. As portrayed in Fig. 9.1(a), the molecules are orientationally disordered. Another possibility is tilt order/disorder. Each hydrocarbon chain in Fig. 9.1(a) is perpendicular to the bilayer surface, but for many lipids the chains are tilted. Also, all-*trans* chains themselves have an orientation, defined by the C—C—C—C plane not indicated in Fig. 9.1(a); this may give rise to chain orientational order/disorder which may be decoupled from headgroup order/disorder. Finally, the rotational isomerism emphasized in the preceding paragraph gives rise to conformational order/disorder.

Lipid/water systems undergo several phase transitions as temperature is changed and as water concentration is changed. (Tardieu *et al.*, 1973; Tristram-Nagle *et al.*, 1987). It is quite likely that most of the kinds of order/disorder mentioned in the preceding paragraph will play a major role in one or several of the observed transitions. However, in this chapter the focus is upon the *main* lipid-bilayer transition. This is the largest of the transitions between two different forms of bilayers, and, of the several transitions of this sort, it is the one that occurs at the highest temperature. In the biophysical literature it is often called the gel-to-liquid-crystalline transition, but this is somewhat inappropriate because both phases are smectic liquid crystals. For the main transition the kind of order/disorder that plays the major role is conformational order/disorder. The X-ray data and the Raman data make it quite clear that conformational order/disorder is important. The size of the entropy of the transition requires many degrees of freedom per molecule that only hydrocarbon chain conformational disorder can supply. Therefore, even though other types of order/disorder may play minor roles in the main transition, the basic picture of this transition is from the states shown in Fig. 9.1(a) to states similar to the ones shown in Fig. 9.1(b). A more detailed discussion of this background information, including the use of experimental data to perform simple thermodynamic tests of the model, has been given by Nagle (1980).

The statistical-mechanical challenge is then to find tractable models that allow conformational order/disorder in chains that interact strongly

with each other and that have a strongly anisotropic boundary condition imposed upon them by the water/head interface. The simple K model provides such a model through a 1–1 isomorphism that is illustrated in Fig. 9.2. The lattice for the chain links is the dual to the brick lattice and is topologically equivalent to the triangular (i.e. hexagonal) lattice. The isomorphism consists of two parts. The first part is between vertical dimers and overlying vertical chain links. The second part is between horizontal dimers and slanted chain links. The vertical chain links therefore carry an energy of 0 and the slanted chain links carry an energy of ε. It is easily verified that the conservation condition on the number of horizontal dimers in each row guarantees that each chain proceeds, albeit in an irregular fashion, vertically through the lattice and that the chain ends may occur only at the top and bottom of the lattice.

The chain-melting model derived from the K model has some major desirable features. The first such feature is that each individual chain has the capability of having one *trans* state and two *gauche* states for each link, just as for actual hydrocarbon chains. However, these possibilities are stringently proscribed by the states of neighbouring chains. Indeed, no two chains can occupy the same lattice site. This is the second desirable feature of the chain model because it includes the excluded-volume interaction between CH_2 groups completely rigorously. The third desirable feature is that anisotropy is built into the model from the start, so this is clearly a model for anisotropic chain melting in membranes rather than a model for isotropic chain melting appropriate for bulk polymers or alkanes. Although the anisotropy is a little stronger in the model than in

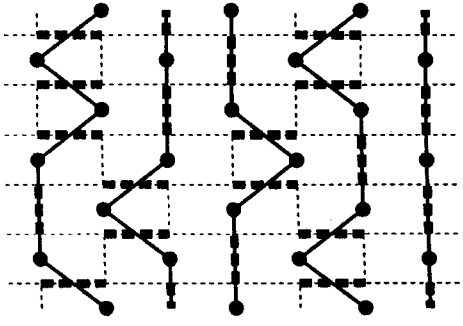

Fig. 9.2 Isomorphism between a state of dimers in the K model on the brick lattice indicated by light dashed lines and a state of anisotropic chains indicated by solid lines on a triangular lattice, with lattice sites shown as large filled circles.

membranes where chains are allowed to reverse their progress along the vertical direction, such reversals would occur rarely.

Not surprisingly, such a simple model also has some undesirable features, as was pointed out when the model was introduced (Nagle, 1973a). Although membranes are thought of as two-dimensional structures for many purposes, and this chain model is clearly a 2-d model, nevertheless, one of the dimensions is not the same. In this chain-melting model the chains are infinitely long along one direction and can only move laterally along one dimension. In contrast, the chains in membranes can move laterally in two dimensions. Even though the chains in membranes are not infinitely long, there are sufficiently many independent units (conformational degrees of freedom) along each chain that it is best to think of the main transition being essentially a 3-d transition. Indeed, this was the motivation for studying the 3-d dimer model discussed in Section 8.† Nevertheless, one still expects a K-type transition for a 3-d model, and there are unlikely to be any new insights gained in comparison with those from the 2-d chain model. The advantage of the 2-d chain model is, of course, the tractability of the mathematics.

A major undesirable feature in the chain model presented in Fig. 9.2 is that every lattice site of the model is occupied by a CH_2 group, so that there is no possibility for the volume of the system to expand. Experiments show, however, that the system does expand in volume. Furthermore, the energy required to do work against the cohesive van der Waals attractive interaction between chains is a substantial fraction (*ca.* 60%) of the total enthalpy of transition (Nagle, 1980). This suggests that there are four principal features that should be included in a chain-melting model for lipid bilayers:

(i) conformational order/disorder;

(ii) excluded-volume interaction;

(iii) anisotropy;

(iv) volume expansions and cohesive interactions.

Except for the anisotropy, similar conclusions have also been drawn for polymer melting transitions (Nagle and Goldstein, 1985).

The basic model in Fig. 9.2 can be modified to accommodate lattice vacancies in the chain model. This is accomplished using the SQK dimer model in Fig. 2.4. The isomorphism to an anisotropic chain model with

†The 3-d model in Section 8 would have an isomeric ratio of 4 *gauche*/1 *trans*, but a different 3-d model that preserves the 2 *gauche*/1 *trans* isomeric ratio has been discussed by Bhattacharjee *et al.* (1983) with similar results.

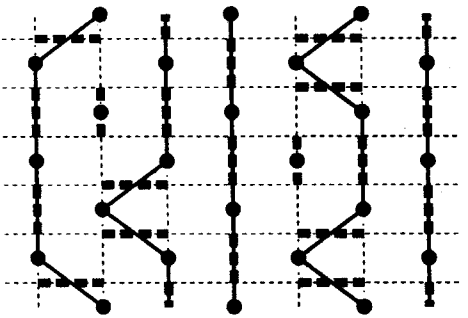

Fig. 9.3 Isomorphism between a state of dimers in the SQK model and a state of anisotropic chains with two vacancies.

some lattice sites vacant is shown in Fig. 9.3. In addition to the two-part isomorphism between the K model and the simple chain model in Fig. 9.2, there is a third part to the isomorphism: whenever a dimer overlies a lattice site of the triangular lattice, no chain passes through that lattice site.

Those vertical bonds on the rectangular lattice for the SQK dimer model that pass through a triangular lattice site are just those that carry an energy δ when occupied by a dimer. Therefore the density of those dimers that correspond to vacancies in the chain model is regulated by δ. In practice, δ is varied so as to vary the chain density ϱ, and the free energy is computed as a function of ϱ. The cohesive energy is then introduced into the model in a ϱ-dependent form as

$$E_{\text{cohesive}} = -a_{\text{vdW}}\varrho^{-b}. \tag{34}$$

This form for the cohesive interactions is basically classical in that local fluctuations are ignored. This is a compromise with the rigour of the statistical mechanics to this point, one that is dictated by the poor prospects for performing detailed r^{-6} interaction calculations rigorously. It may be noted, however, in view of the fact that classical or mean-field calculations are best for very-long-range potentials, that the rigour is placed on the proper part of the model, namely the nearest-neighbour excluded-volume part, and the long-range van der Waals interactions are the ones best approximated classically. The best value of the exponent b is not altogether clear, with various arguments yielding values in the range 1–2.5† (Nagle, 1973a); the results are not highly sensitive to values

†Cotter (1977) has pointed out that $b = 1$ is the only value strictly consistent with mean-field theory.

of b in this range. The overall strength of the cohesive interactions a_{vdW} is known experimentally to some precision for 3-d systems. For each temperature the thermodynamically stable state is determined by finding the value of ϱ for which the free energy per chain link is lowest.

The results of the calculations are rather encouraging. By allowing for volume expansion against cohesive attractive forces, the transition becomes first-order. In the first calculations the value of a_{vdW} was taken to yield the heat of sublimation of 3-d hydrocarbon chain systems, which resulted in transitions that were too small. This choice, however, is inappropriate for a 2-d model, for which each chain is surrounded by only two other chains rather than six as in the 3-d system. Reducing a_{vdW} by a factor of 3 gives results for the enthalpy of transition, the volume change, the change in surface density of the lipids (surface area per lipid) and the transition temperature that are in reasonable (*ca.* ±25%) agreement with experiment (Nagle, 1986).

At this point the reader may have the impression that, while the preceding development is certainly an application of dimer models, the K-type transition has disappeared from the picture. In fact, the effects of the K-type transition are still felt above the first-order transition in the form of elevated fluctuations that may be responsible for the enhanced permeability of lipid bilayers above the transition temperature T_M (Nagle and Scott, 1978). In Section 10 we shall see that the K-type transition has just moved into a different part of the phase diagram.

There have been many theoretical papers dealing with the main transition in lipid bilayers—far too many to review here. Many of the earlier papers were reviewed by Nagle (1980). Subsequent papers of particular interest from the point of view of this chapter include that of O'Leary (1981), in which the chain-melting lattice model is combined with a lattice decoration scheme to allow the inclusion of anaesthetics, and the papers of Izuyama and Akutsu (1982a,b) reviewed in Section 8.

10 Order parameter, anisotropic field, and application to monolayers

Up to this point in this chapter the focus on thermodynamic properties has been on the specific heat or the energy or the free energy. It is customary, when discussing spin-type models or vertex models, to give equal attention to the order parameter, such as the spontaneous magnetization, and to the conjugate ordering field, such as the magnetic field. The reason why equal attention has not been paid to similar quantities for the dimer models with K-type transitions is simply that it

is far from apparent what the related quantities are for these models. The obvious attempt to find an order parameter for the low-temperature phase of the K model would be to consider the density of vertical dimers, perhaps with a constant such as $\frac{1}{3}$ subtracted. Any quantity involving densities of dimers, however, while being non-zero in the ordered low-temperature phase, where the order parameter ought to be non-zero, is also non-zero for all but a few temperatures above T_K, where a proper Landau order parameter should be identically zero. Similarly, the obvious attempt to include an ordering field is to favour vertical dimers versus horizontal dimers by an additional energy δ, but this just changes the single energy parameter from ε to $\varepsilon + \delta$.

In the field of physisorption to be discussed in more detail in Section 11, this issue has been dealt with by focusing on the high-temperature phase and describing the density of domain walls as vanishing near T_K as $t^{\bar{\beta}}$, where $\bar{\beta} = \frac{1}{2}$. This choice of notation for the critical exponent suggests that the density of domain walls is a kind of order (or disorder) parameter. However, since the specific heat is just proportional to the derivative of the density of domain walls, $\bar{\beta}$ is trivially related to the specific-heat exponent α by $\bar{\beta} = 1\text{-}\alpha$, and so this does not add a second pair of conjugate variables to the model. The use of the bar over β does emphasize the main point of the preceding paragraph, namely that the K-type phase transition is unusual when compared with spin- or vertex-type transitions.

A different perspective regarding a second pair of conjugate thermodynamic variables has been obtained in the course of applying the models in Section 9 to monolayers of lipids or general surfactants. Since those models involve only one layer of chains rather than the two layers that exist in bilayers, they should be at least as good for monolayers as for bilayers.† A most important advantage of doing monolayer experiments in the laboratory is that a very natural pair of thermodynamic variables is available, namely the surface area per molecule A and the lateral surface pressure π. Indeed, the most popular experimental way to induce the main phase transition in monolayers is to vary π isothermally.‡

† Of course, just as for bilayers, the models would not be expected to yield all the transitions in monolayers, such as the 2-d liquid-to-vapour transition or the 2-d solid transitions that seem to occur in monolayers at the densest coverages.

‡ The experimental literature is especially confusing regarding the determination of the thermodynamic order of the phase transition observed by π–A isotherms, with many of the results not having flat portions consisting of A changing at constant π as demanded by a first-order transition. It has been concluded by one of the authors (Nagle, 1986) that the monolayer transition is basically standard first-order. Since then, especially clean isotherms that show flat portions have been generated for DPPC and pentadecanoic acid by Hifeda and Rayfield (Hifeda, 1988) so the issue will be considered resolved in this chapter.

Although the main transition may also be induced in bilayers by increasing the isotropic pressure P isothermally, the size of the transition varies little when this is done at different temperatures. In contrast, the size of the isothermal discontinuity in A in monolayers decreases substantially as T is increased, suggesting the approach to a critical point. Unfortunately, such critical points, if they exist, would occur at values of π too large for mechanical stability of the monolayers studied. Nevertheless, the experiments are suggestive that π and A are the variables that play the role of ordering field and order parameter, and this view is supported by the calculations to which we now turn.

Since the methods and the results are qualitatively the same for the simpler chain model corresponding to the basic K model as for the more realistic chain model corresponding to the SQK model, let us consider it for simplicity. The area per chain A, which is a linear distance along the horizontal direction in Fig. 9.2, is proportional to $(2-\varrho_x)^{-1}$, where ϱ_x is the density of horizontal dimers, which can vary from 0 to 1. Given T and π, the thermodynamic value of A is determined by minimizing the free energy per chain link given by

$$g = \varrho_x \varepsilon - TS + \pi A \tag{35}$$

with respect to A. This calculation is possible because the entropy S depends only upon the density of horizontal dimers. That is to say, the entropy is the same for two different states with different values of π and T, provided that both states have the same value of ϱ_x and therefore of A. This is a special property of systems whose interactions are exclusively the all-or-nothing excluded-volume interaction. Therefore the exact calculation of the usual free energy with $\pi = 0$,

$$f = -kT \ln Z = \varrho_x \varepsilon - TS, \tag{36}$$

enables one to calculate S for a given value of T. The exact calculation also yields ϱ_x. By systematically varying T in (36), the entropy S is obtained as a function of ϱ_x. These values of $S(\varrho_x)$ are then used in (35), where, of course, T is not the same as in (36) and π is not zero. Further details of the calculation are provided in Nagle (1975a,b).

The results of the calculation are shown schematically in Fig. 10.1. In this figure steeply rising isotherms are drawn for $A < 1$. In fact, the model does not allow chains to be packed more closely together than $A = 1$, so, strictly speaking, these isotherms should all be vertical and lie on top of one another. Since this is visually difficult, and since it is due only to a minor omission in the model (namely lattice compressibility), artistic licence has been employed in Fig. 10.1 for $A < 1$. For $T > T_K$ the isotherms in Fig. 10.1 are monotonically decreasing and the only transition is a weak second-order one at $A = 1$. As T decreases toward

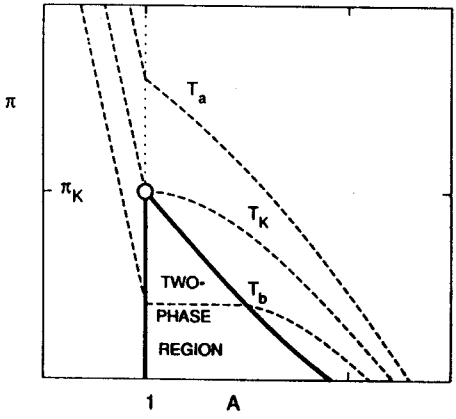

Fig. 10.1 The π–A phase diagram for the chain-melting models of Section 9. The dashed lines show three isotherms for $T_a > T_K$, T_K and $T_b < T_K$. The boundary of the two-phase region is shown by bold solid lines ending in a critical point indicated by an open circle. The isotherms in the ordered phase ($A < 1$) have been drawn with finite slope instead of infinite slope for visual clarity and to accommodate non-zero lattice compressibility not included in the model.

T_K, the slope of the isotherms approaches zero at $A = 1$. For T below T_K the slope of each isotherm becomes zero for a value of $A_m > 1$ and is negative for $1 < A < A_m$. This corresponds to a typical van der Waals loop, except that the loop has a discontinuous derivative at $A = 1$, and there is a region in the π–A plane where each putative homogeneous thermodynamic state has a higher value of g than the heterogeneous state consisting of a mixture of states with the same value of π and the values of $A = 1$ and $A = A_F > A_m$. The values $A = 1$ and A_F, of course, mark the boundaries of the two-phase region depicted in Fig. 10.1.

In the calculations described in Section 9, π was implicitly set equal to zero, so only a one-dimensional slice of the phase diagram in Fig. 10.1 was obtained. For the chain model with no vacancies corresponding to the simple K model this slice encountered the K-type transition at T_K because π_K is 0. For the chain model with vacancies corresponding to the SQK model the two-phase region essentially slides up the π axis with fairly minor shape changes, so $\pi_K > 0$, and the $\pi = 0$ slice yields a first-order transition. However, the model still has a K-type transition, which is a special critical point in the extended phase diagram in Fig. 10.1. Furthermore, the critical fluctuations that become infinite as the critical point at T_K and π_K is approached are still significant as the first-order transition is approached at values of π near to but not equal to π_K.

The phase diagram in Fig. 10.1 makes the K model look a little more normal in so far as there is a two-phase region that ends at some kind of critical point and there is a pair of conjugate thermodynamic variables, π–A, in addition to S–T. The critical point is, however, still abnormal. If one supposes that the discontinuity in the order parameter is proportional to the discontinuous change ΔA then the critical exponent β, defined by $\Delta A \sim t^{\beta}$, equals 1. With this identification, the other critical exponents become $\gamma = 1 = \gamma'$, $\delta = 2$ and $\alpha = \alpha' = 0$ (finite) (Nagle, 1975a). These exponents obey the thermodynamic inequalities, such as $\alpha' + 2\beta + \gamma' \geq 2$ (Rushbrooke, 1963), but not the scaling identities.

Technically, the critical point in Fig. 10.1 is reminiscent of a tricritical point (Griffiths, 1970) because it is the point in the π–T plane where a first-order transition changes to a continuous transition. It is, however, considerably different from the classical tricritical points found in spin-type systems, for two reasons. First, the continuous transition exhibits only a weak discontinuity in the lateral compressibility $-A^{-1}(\delta A/\delta\pi)_T$ instead of a strong divergence. Secondly, the critical exponents are considerably different from the usual tricritical exponents. Also, to exhibit a typical tricritical point with three critical lines meeting at it would require yet another pair of conjugate thermodynamic variables. Perhaps, with such an additional pair of variables, it would be possible to resolve the two aforementioned differences by redefining the order parameter and the ordering field.†

At this time it seems that the phase diagrams for models with K-type transitions are quite different from the conventional phase diagram obtained for simple magnetic or fluid systems. Nevertheless, the identification of the π–A variables at least yields a comparable kind of phase diagram. Most importantly, it allows an application of the models to monolayer systems and gives deeper insight into the bilayer phase transition.

11 Application to 2 × 1 commensurate–incommensurate transitions

A number of new kinds of phases and phase transitions have emerged from the field of physiadsorption of simple atoms to crystalline surfaces.

†It should be noted that a considerably different way to define an ordering field for the high-temperature phase has been advanced by Huse and Fisher (1984). This definition requires distinguishing alternating A- and B-type domains and the field favours one type over the other. Unfortunately, it has not so far been possible to implement this field in exact dimer calculation. Using a phenomenological theory, Huse and Fisher calculate a susceptibility exponent $\gamma = \frac{3}{2}$.

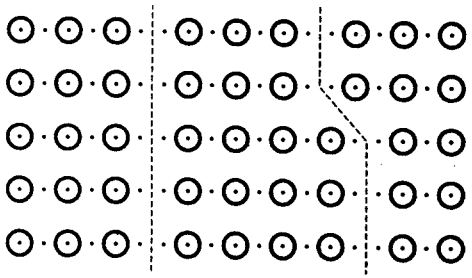

Fig. 11.1 Sketch of a 2 × 1 incommensurate phase. Each adsorbed atom is represented as a large open circle. Each site of minimum potential energy on the crystalline substrate is represented as a small dot. The state shown has two domain walls indicated by dashed lines.

The particular kind of phase discussed here is characterized as a striped incommensurate phase. An example is sketched in Fig. 11.1 for a substrate that is spatially anisotropic. The underlying crystalline substrate is supposed to consist of sites of potential energy minima for the adsorbed atoms. If the y spacing of the substrate is nicely commensurate with the energetically preferred spacing of nearest-neighbour adsorbate atoms then the adsorbed atoms will tend to line up in vertical rows. However, if the potential minima in the horizontal direction are spaced too close together for nearest-neighbour occupancy of the adsorbate atoms then one or more sites on the substrate will be vacant. In the example in Fig. 11.1 it is supposed that there is also an attractive force that favours occupancy of alternate sites in the horizontal direction. Furthermore, the mean coverage of the surface is affected by the vapour pressure/chemical potential of the adsorbate. In the example in Fig. 11.1 it is supposed that the vapour pressure is too low for coverage of half the sites of the substrate and that the preferred defects consist of occasional larger spacing of atoms in the horizontal direction. Going from row to row, these larger spacings will tend to occur at the same value of x so as to minimize the interaction energy in the vertical direction between adsorbate atoms on adjacent rows. These larger spacings therefore form domain walls, which are indicated in Fig. 11.1 by dashed lines. Nevertheless, entropy demands that there be some wandering in the x direction of the domain walls, as illustrated by the wall to the right in Fig. 11.1. The domains on either side of each wall are distinguished by the adsorbate atoms sitting on one of two (or p in general) different sublattices of minimum substrate potential. In the terminology used in this field the entire state shown in Fig. 11.1, including both types of domains and the domain walls, is a single $p \times 1$ incommensurate phase (with $p = 2$) and not a mixture of

coexisting crystalline phases, as the term "domain wall" might suggest. As the surface coverage increases, the concentration of domain walls decreases and a transition occurs into a commensurate phase in which all x spacings equal the smallest ones shown in Fig. 11.1 and all atoms sit on just one of the two sublattices. For more details and reviews of the experimental systems the reader may consult more extensive reviews (Fisher, 1984, 1986; den Nijs, 1988).

Figure 11.2 shows how the 2×1 state in Fig. 11.1 corresponds to the K model. A brick lattice is superimposed upon the rectangular lattice of Fig. 11.1. Regions of vertical dimers in Fig. 11.2 correspond to regions in which the adsorbed atoms are regularly spaced in the 2×1 pattern. Strings of horizontal dimers in Fig. 11.2 correspond to the domain walls in Fig. 11.1. One notices, however, that the domain walls in Fig. 11.2, indicated by light dashed lines, are not drawn identically with the ones in Fig. 11.1. This emphasizes that the correspondence between the K model and the most physical adsorbed 2×1 model is not one-to-one. In particular, each domain wall in the K model must wander to the right or the left upon proceeding from row to row, whereas domain walls in the most physical 2×1 model may proceed straight up or may, with an extra energy, wander to either the left or the right as they proceed from row to row. Therefore, while every state of the K model corresponds to a state of the adsorbed 2×1 model shown in Fig. 11.1, there are additional states in the physical model and the states have different energies.

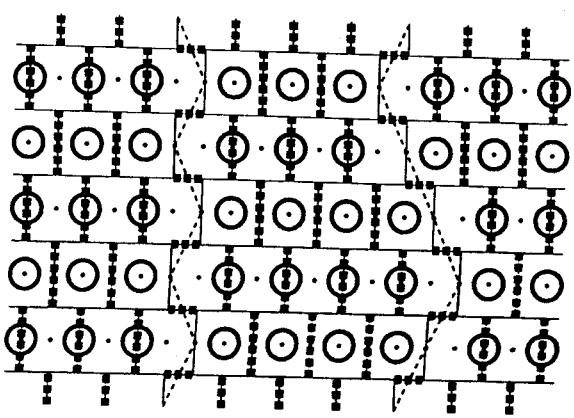

Fig. 11.2 Correspondence between the 2×1 adsorbed atom model in Fig. 11.1 and the K model. The underlying brick lattice for the K model is shown with solid lines, and the dimers are shown with heavy dashed lines. The two domain walls are indicated by light dashed lines.

In this paragraph we argue that the differences emphasized in the preceding paragraph between the K model and the physical 2 × 1 model should be inconsequential for phase-transition behaviour because they belong to the same universality class. Both models have the three important properties that the walls

(i) cannot terminate,

(ii) cannot cross,

(iii) can wander in the x direction.

The details of the wandering, that is (a) the number of directions for wall wandering at each level and (b) the energy of the different directions, are local properties much like the local coordination number and the local interaction strengths in spin models. Such details would not be expected to affect the nature of long-range correlations or the universality class of transitions.

As the surface coverage increases with increasing chemical potential of the adsorbate, the density of domain walls decreases and vanishes at some chemical potential μ_K as $(\mu_K - \mu)^{\tilde{\beta}}$, where $\tilde{\beta} = \frac{1}{2}$ is the now-familiar critical exponent of the K-type transition. This result supports the analysis of Pokrovsky and Talapov (1979) and many others (den Nijs, 1988) for the critical behaviour of striped commensurate–incommensurate phase transitions.

There are three additional features that may appear, individually or in combination, in striped incommensurate 2 × 1 phases. These features are shown in Fig. 11.3. The first feature is a second type of domain wall in which nearest-neighbour sites in the x direction are occupied. It is common to call this a heavy wall, in contrast with the light walls portrayed in Figs. 11.1 and 11.2. The second feature is that heavy and light walls may meet and annihilate or be created at a dislocation. The third feature is that like walls, such as two light walls, may also be annihilated or created at a dislocation that is more costly in energy.

Combinations of these three additional features are present in some of the exactly solved dimer models presented earlier in this chapter. The 4–8/2/1 model has two kinds of domain walls, each of which may annihilate with one of the other type, but not with one of the same type. The domain-wall picture of the 4–8/2/1 model can be seen in Fig. 3.1. Figure 3.1 does not indicate the correspondence to an adsorbed-atom model, so it is not obvious that the two kinds of walls there are heavy and light; this becomes obvious in Fig. 11.4, which will be discussed in the next paragraph in connection with the 4–8s/2/1 model. As was discussed in

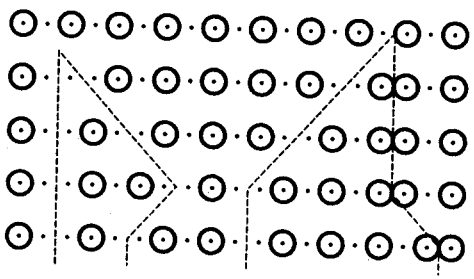

Fig. 11.3 Three possible additional features of striped phases. On the far right is shown a heavy domain wall. This heavy domain wall annihilates with a light domain wall at the upper right. At the upper left is shown annihilation of two light domain walls.

Section 5, the 4–8/2/1 model has two phase transitions. The lower one is a K-type transition into a striped incommensurate phase with a density of heavy walls that is different from the density of light walls. The upper transition is an inverted K-type transition into a disordered phase whose correlation functions are still not well characterized. It is possible that this high-temperature phase is a commensurate disordered phase of the sort described by Kardar and Shankar (1985) using the free-fermion

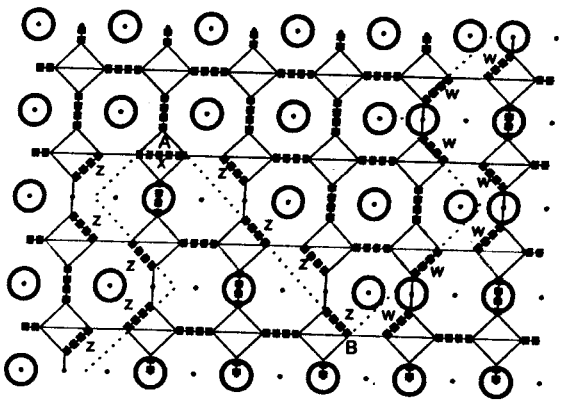

Fig. 11.4 Correspondence between the 4–8s/2/1 dimer model and an adsorbed-atom model with heavy and light domain walls and with dislocations of two types. Dimers not in the ground state are indicated by their activities w, x or z. Domain walls are indicated by light dashed lines. Two light walls annihilate at A, and a light wall and a heavy wall are created at B. Adsorbed atoms are indicated by large open circles centred on the substrate lattice indicated by small dots.

method, which, however, only yields an approximation to their model.

The 4–8s/2/1 model has all the features of the 4–8/2/1 model, and additionally it has the feature that like walls can annihilate as shown at location A on the left-hand side of Fig. 11.4. Like the 4–8/2/1 model, the 4–8s/2/1 model has two transitions, but both transitions are O-type rather than K-type, which shows the critical importance of like-wall dislocations on the universality class of transitions in 2 × 1 striped systems. In the limit when one of the two types of walls is prohibited ($w \to \infty$ in Fig. 11.4) the 4–8s/2/1 model reduces to the 3–12/1 model. In this case like-wall annihilation is still allowed, but there is only one O-type transition (Bhattacharjee, 1984).

In the field of physisorption multicriticality and crossover behaviour are very important. In the conventional picture in this field relaxation of the domain wall conservation condition by allowing like-wall dislocations is relevant in changing the transition behaviour of $px1$ models from K-type to O-type if and only if $p = 1$ or 2 with crossover exponent $\phi = (6\text{-}p^2)/4$ (Huse and Fisher, 1984). The exact calculations for the 3-12/1 and the 4-8s/2/1 models show that like-wall dislocations are indeed relevant. Furthermore, the value of $\phi = 1/2$ calculated for the 3-12/1 model by Bhattacharjee (1984) strongly suggests that the closely related set of models consisting of the K, 3-12/1, 4-8/2/1 and 4-8s/2/1 models should be viewed as $p = 2$ models as has been implied by Figures 11.2 and 11.4. In this picture the K-type transition becomes a multicritical point at the end of a line of O-type transitions in a phase diagram that includes the like-wall dislocation energy as a parameter. On the other hand, the 4-8/2/1 model exhibits an example where an O-type transition is a multicritical point which occurs at the intersection of a K-type transition and an inverted K-type transition (Nagle and Yokoi; 1987) with $\phi = 1$, so it seems inadvisable to make overgeneralizations regarding which kind of transition behaviour should be the special multicritical point and which should be the more generally obtained one.

Except for the result mentioned at the end of the preceding paragraph, each of the preceding results was anticipated by free-fermion approximations (reviewed by den Nijs, 1988) or by random-walk arguments (reviewed by Fisher, 1984, 1986), both of which have wider applicability than the dimer models that have been presented. The value of the K-type models in this context is that they are precisely defined classical statistical-mechanical models that can be solved exactly and that are in the same universality class as the more-physical models for the phenomena. The fact that the exact calculations yield the same results as the other methods provides a firm underpinning for more-extensive theories of striped incommensurate systems and their phase transitions.

12 Concluding remarks

Dyson (1988) has recently emphasized the tension between the science of unification, which he associates with Athens, and the science of the particular, which he associates with Manchester. From this perspective this chapter is more Mancunian than Athenian. This accords with the belief that complex cooperative phenomena require careful attention to detail to avoid the overgeneralization that accompanied the classical era of mean-field theories. Accordingly, we have focused upon a subset of exactly solvable two-dimensional models that embody the property of anisotropy, upon expanding that subset by considering many new models in Sections 2 and 5, and upon emphasizing the differences between K-type and O-type transitions and the features of models that produce the two types.

We have not, however, been impervious to the appeal of Athenian unification. In Section 10 an attempt was reviewed to enlarge the phase diagram of the K model so as to make it look more similar to the phase diagram of magnets and fluids. Also, in Section 8 the extension of these models to three dimensions was reviewed, and in Section 7 finite-size scaling theory was shown to be correct when suitably extended. Most important, in our opinion, is the application of these dimer models to widely disparate phenomena. These applications relate the main lipid-bilayer phase transition, the monolayer chain-melting transition, and striped commensurate–incommensurate transitions to each other, and so a higher unity of phenomena is obtained.

Finally, we should like to emphasize our appreciation of exact statistical-mechanical methods for cooperative phenomena. Such methods, if carried out carefully, eliminate any uncertainty in the calculations and thereby allow more definitive conclusions. If the Pfaffian-dimer technique employed in this chapter is representative then such methods have long half-lives and far-reaching applications. However, to return to the Mancunian theme, it is important that exact solutions not be applied indiscriminately to phenomena. It is unreasonable to try to describe everything in the universe in terms of the Ising model. We hope that the reader is convinced that phenomena such as the main phase transition in lipid bilayers or the striped commensurate–incommensurate transitions in physisorbed systems are better described by models in which anisotropy plays a fundamental role, as it does in the dimer models discussed in this chapter.

References {with author index}

Barber, M. N. (1983). *Phase Transitions and Critical Phenomena,* Vol. 7 (ed. C. Domb and J. L. Lebowitz), p. 146. Academic Press, London. {274}

Baxter, R. J. (1973). *J. Stat. Phys.* **9,** 145. {245}

Bhattacharjee, S. M. (1984). *Phys. Rev. Lett.* **53,** 1161. {244, 269, 294}

Bhattacharjee, S. M. and Nagle, J. F. (1985). *Phys. Rev.* **B31,** 3199. {244, 274, 276}

Bhattacharjee, S. M., Nagle, J. F., Huse, D. A. and Fisher, M. E. (1983). *J. Stat. Phys.* **32,** 361. {279, 283}

Cotter, M. A. (1977). *Mol. Cryst. Liq. Cryst.* **39,** 173. {284}

den Nijs, M. (1988). *Phase Transitions and Critical Phenomena,* Vol. 12, (ed. C. Domb and J. L. Lebowitz), p. 219. Academic Press, London. {291, 292, 294}

Dyson, F. J. (1988). *Infinite in All Directions.* Harper and Row, New York {295}.

Elser, V. (1984). *J. Phys.* **A17,** 1509. {253}

Ferdinand, A. E. and Fisher, M. E. (1969). *Phys. Rev.* **185,** 832. {276}

Fisher, M. E. (1966). *J. Math. Phys.* **7,** 1776. {244}

Fisher, M. E. (1984). *J. Stat. Phys.* **34,** 667. {291, 294}

Fisher, M. E. (1986). *J. Chem. Soc. Faraday Trans. 2* **82,** 1569. {272, 291, 294}

Fisher, M. E. and Stephenson, J. (1963). *Phys. Rev.* **132,** 1411. {271}

Fowler, R. H. and Rushbrooke, G. S. (1937). *Trans. Faraday Soc.* **33,** 1272. {236}

Griffiths, R. B. (1970). *Phys. Rev. Lett.* **24,** 715. {289}

Hartwig, R. E. and Stephenson, J. (1968). *J. Math. Phys.* **9,** 425..{271}

Hifeda, Y. M. (1988). Fatty Acid and Lipid Monolayers on Air–Water Interfaces. Thesis, University of Oregon. {286}

Huse, D. A. and Fisher, M. E. (1984). *Phys. Rev.* **B29,** 239. {289, 294}

Izuyama, T. and Akutsu, Y. (1982a). *J. Phys. Soc. Japan* **51,** 50. {278, 279, 285}

Izuyama, T. and Akutsu, Y. (1982b). *J. Phys. Soc. Japan* **51,** 3449. {278, 285}

Kardar, M. and Shankar, R. (1985). *Phys. Rev.* **B29,** 239. {293}

Kasteleyn, P. W. (1961). *Physica* **27,** 1209. {252}

Kasteleyn, P. W. (1963). *J. Math. Phys.* **4,** 287. {236, 239, 244, 246, 253}

Kitahama, K. and Kiriyama, H. (1977). *Bull. Chem. Soc. Japan* **50,** 3167. {245}

Kornilov, E. I. and Priezzhev, V. B. (1984). *Z. Phys.* **B54,** 351. {279}

McCoy, B. M. and Wu, T. T. (1973). *The Two-Dimensional Ising Model,* Harvard University Press, Cambridge, Massachusetts. {253, 273}

McMullen, R. K., Thomas, R. and Nagle, J. F. (1982). *J. Chem. Phys.* **77,** 537. {241}

Matsuo, T., Masaharu, O., Suga, H., Seki, S. and Nagle, J. F. (1974). *Bull. Chem. Soc. Japan* **47,** 57. {245}.

Montroll, E. W. (1964). *Applied Combinatorial Mathematics* (ed. E. F. Beckenback), Chap. 4. Wiley, New York. {251, 253}

Montroll, E. W. (1969). *J. Math. Phys.* **10,** 753. {279}

Nagle, J. F. (1969a). *J. Chem. Phys.* **50,** 2813. {245}

Nagle, J. F. (1969b). *Commun. Math. Phys.* **13,** 62. {248}

Nagle, J. F. (1973a). *J. Chem. Phys.* **58,** 252. {283, 284, 285}

Nagle, J. F. (1973b). *Proc. Natl Acad. Sci. USA* **70,** 3443. {239}

Nagle, J. F. (1975a). *Phys. Rev. Lett.* **34,** 1150. {239, 240, 287, 289}

Nagle, J. F. (1975b). *J. Chem. Phys.* **63,** 1255. {287}

Nagle, J. F. (1980). *Ann. Rev. Phys. Chem.* **31,** 157. {281, 283}
Nagle, J. F. (1986). *Faraday Discuss. Chem. Soc.* **81,** 151. {285, 286}
Nagle, J. F. and Allen, G. R. (1971). *J. Chem. Phys.* **55,** 2708. {241}
Nagle, J. F. and Goldstein, M. (1985). *Macromolecules* **18,** 2643. {283}
Nagle, J. F. and Scott, H. L. (1978). *Biochim. Biophys. Acta* **513,** 236. {285}
Nagle, J. F. and Yokoi, C. S. O. (1987). *Phys. Rev.* **B35,** 5307. {245, 267, 294}
Nienhuis, B., Hilhorst, H. J. and Blote, H. W. J. (1984). *J. Phys.* **A17,** 3559. {243}
O'Leary, T. J. (1981). *Biophys. Chem.* **13,** 315. {285}
Onody, R. N. and Kurak, V. (1988). *Phys. Rev.* **B38,** 5061. {245}
Onsager, L. (1944). *Phys. Rev.* **65,** 117. {236, 255}
Pokrovsky, V. L. and Talapov, A. L. (1979). *Phys. Rev. Lett.* **42,** 65. {239, 292}
Priezzhev, V. B. (1981). *J. Stat. Phys.* **26,** 817. {277}
Rokhsar, D. S. and Kivelson, S. A. (1988). *Phys. Rev. Lett.* **61,** 2376. {270}
Rushbrooke, G. S. (1963). *J. Chem. Phys.* **39,** 842 {289}.
Salinas, S. R. and Nagle, J. F. (1974). *Phys. Rev.* **B9,** 4920. {245, 273}
Schultz, H. J. (1980). *Phys. Rev.* **B22,** 5274. {272}
Sutherland, B. (1968). *Phys. Lett.* **26A,** 532. {273}
Tardieu, A., Luzzati, V. and Reman, F. C. (1973). *J. Mol. Biol.* **75,** 711. {281}
Temperley, H. N. V. and Fisher, M. E. (1961). *Phil. Mag.* **6,** 1061. {252}
Thompson, C. J. (1972). *Mathematical Statistical Mechanics.* Princeton University Press. {253}
Tristram-Nagle, S., Wiener, M. C., Yang, C.-P. and Nagle, J. F. (1987). *Biochemistry* **26,** 4288. {281}
Wu, F. Y. and Lin, K. Y. (1975). *Phys. Rev.* **B12,** 419. {245}
Yokoi, C. S. O., Nagle, J. F. and Salinas, S. R. (1986). *J. Stat. Phys.* **44,** 729. {241, 272}
Youngblood, R. and Kjems, J. K. (1979). *Phys. Rev.* **B20,** 3792. {245}